Applied Physics A (2024) 130:350
https://doi.org/10.1007/s00339-024-07501-y

Applied Physics A
Materials Science & Processing

INVITED REVIEW

Ultraviolet photodetectors based on wide bandgap semiconductor: a review

Jijun Ding[1] · Pengfei Zhao[1] · Haixia Chen[1] · Haiwei Fu[1]

Received: 17 January 2024 / Accepted: 2 April 2024 / Published online: 29 April 2024

Abstract

Ultraviolet (UV) photodetectors (PDs) are effective devices that convert UV radiation energy into electrical signals, and they are widely used in aerospace, chip manufacturing and other fields. At present, the design and manufacture of UV PDs based on wide bandgap semiconductor materials is also an important branch of optoelectronics technology. Wide bandgap semiconductor materials with strong UV absorption, high carrier mobility, exciton binding energy, and temperature resistance, have become ideal materials for fabricating high-performance UV PDs. Meanwhile, some novel materials have also been found to be suitable for the fabrication of UV optoelectronic devices in recent years, such as chalcogenide materials, double-layer hydroxide materials, and graphene-based materials. In this review, the research progress performance parameters, structures and commonly used materials of UV PDs is systematically introduced. In addition, the methods for optimizing device performance based on various property effects of materials are discussed in detail. The broad research prospect of some novel materials and corresponding application in UV PDs are explored, which provide a reference for future research and development of UV PDs.

Keywords Ultraviolet photodetectors · Wide bandgap semiconductor · Structures · Performance

1 Introduction

Solar spectra mainly contain 5% ultraviolet (UV), 50% visible, and 45% infrared light wavelength. UV also refers to specific electromagnetic radiation in the wavelength range of 10–400 nm [1], which can be divided into UVA, UVB, UVC and VUV, and its corresponding wavelengths are 320–400 nm, 280–320 nm, 100–280 nm and 10–200 nm, respectively [2–8], as is shown in Fig. 1. Different wavelengths of UV light have different effects. Such as, excessive exposure to UV radiation will cause the skin redness and swelling, accelerate skin aging, and even lead to skin cancer [9, 10]. However, moderate UV can activate vitamin D synthesis, eliminate various bacteria, supplement calcium and help emotional healing [5, 11, 12]. UV light with wavelengths ranging from 240 to 280 nm can be used to kill bacteria, extreme ultraviolet can be used for high-precision photolithography machine in chip manufacturing. It is necessary to detect the intensity of UV radiation. UV photodetectors (PDs) can convert UV radiation into electrical signal [13]. It has extensive applications in medicine, astronomy, environmental monitoring, missile detection, ozone hole monitoring and other aspects of daily life, military and industrial development [14–17]. Therefore, researchers are committed to manufacturing high-performance UV PDs.

High-performance UV PDs have high sensitivity, ultrafast response, low power consumption and ultrahigh on/off ratio [18–20]. To meet these requirements, wide bandgap semiconductors, such as ZnO, GaN and Ga_2O_3, are often used for UV PDs due to high electron mobility, strong absorption of UV radiation and good stability [21, 22]. Generally, traditional UV PDs are fabricated on silicon or sapphire, limiting their application in certain field [23, 24]. With the development of technology, novel optical sensing technologies has new requirements, such as high compatibility, flexible and wearable, allowing for fewer aberrations and adapted to different surfaces to enable new functionalities with greater

✉ Jijun Ding
jjding@xsyu.edu.cn

[1] Shaanxi Engineering Research Center of Oil and Gas Resource Optical Fiber Detection, Shaanxi Key Laboratory of Measurement and Control Technology for Oil and Gas Wells, College of Science, Xi'an Shiyou University, Xi'an 710065, China

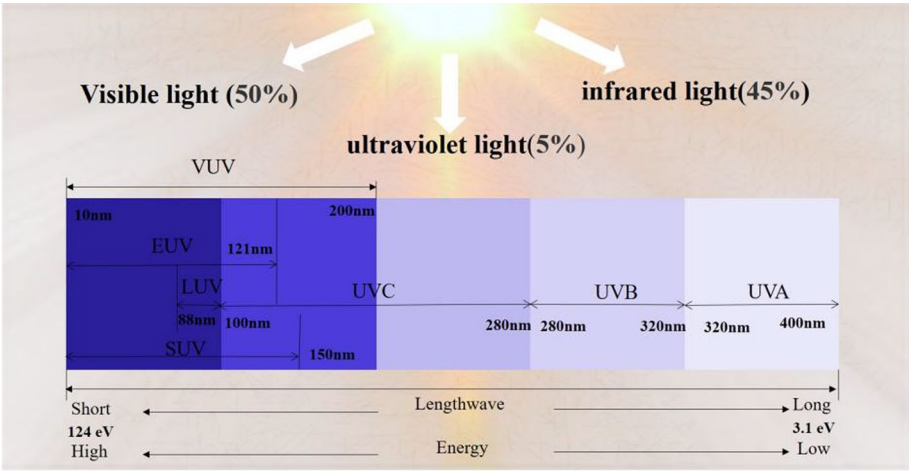

Fig. 1 Ultraviolet Classification

potential [25–27]. In recent years, biological DNA molecules and other biomass materials have also been gradually applied to PDs, and the roles in device performance has attracted widespread attention.

In recent years, some researchers have focused on the discussion of UV PDs, which lays a solid foundation for the preparation of future UV PDs. Zou et al. [28] summarized main detection parameters, working principle and structure of UV PDs, the current technological status and related new detectors suitable for wide bandgap semiconductor materials in the past 5 years. Hao et al. [20] reported the detection technology of deep UV radiation in the range of 190–350 nm, highlighting the advantages of wide-bandgap semiconductor materials in the detection of deep UV radiation. Ouyang et al. [29] found that ZnO nanowires provide a reliable basis for self-powered UV PDs devices in the future due to large surface-area ratios and the deep surface defects, which greatly improves the device sensitivity and responsiveness.

In this review, we systematically summarize the main performance parameters, various design structures, novel materials, and various performance effects as well as applications. In addition, the advantages and disadvantages of various design structures and commonly used detector materials are analyzed, and novel self-powered and wearable UV PDs are discussed.

2 Parameters of ultraviolet detector

The application of UV sensors covers industrial, military, environmental monitoring, and electronic equipment manufacturing, resulting in a huge demand for UV PDs. To accurately and effectively evaluate the performance of UV PDs, it must be judged based on relevant parameters. Some parameters of ultraviolet detector are shown in Fig. 2, including photocurrent, dark current, sensitivity, response/recovery time, quantum efficiency, detectability, light harvesting efficiency, and mechanical flexibility, etc.

2.1 Photocurrent (I_{ph}) and dark current (I_{dark})

Photocurrent is usually the current generated in the presence of light, while dark currents are generated under dark conditions, which is mostly caused by material defects. When the dark current is ultralow, it indicates that the material has a high crystallization and good performance. Therefore, it is necessary to combine doping or coating methods to shield defects in the sample preparation process, reducing the recombination of photo-generated carriers.

2.2 Sensitivity (S)

Sensitivity (S) is used to evaluate the ability of the PDs to respond to UV radiation, which is defined as the ratio of the difference between photocurrent and dark current. The higher the crystallinity of semiconductor, the lower the dark current and the higher the sensitivity.

$$S = \frac{\Delta I}{I_d} = \frac{I_{ph} - I_d}{I_d} \tag{1}$$

2.3 Responsivity (R)

Responsivity (R) can also reflect the response of the PDs to UV radiation, which denotes the ratio of photocurrent to incident optical power density of radiation at a certain bias voltage [30]:

$$R = \frac{\Delta I}{PS} \tag{2}$$

where P denotes the light intensity, and S denotes the effective irradiation area.

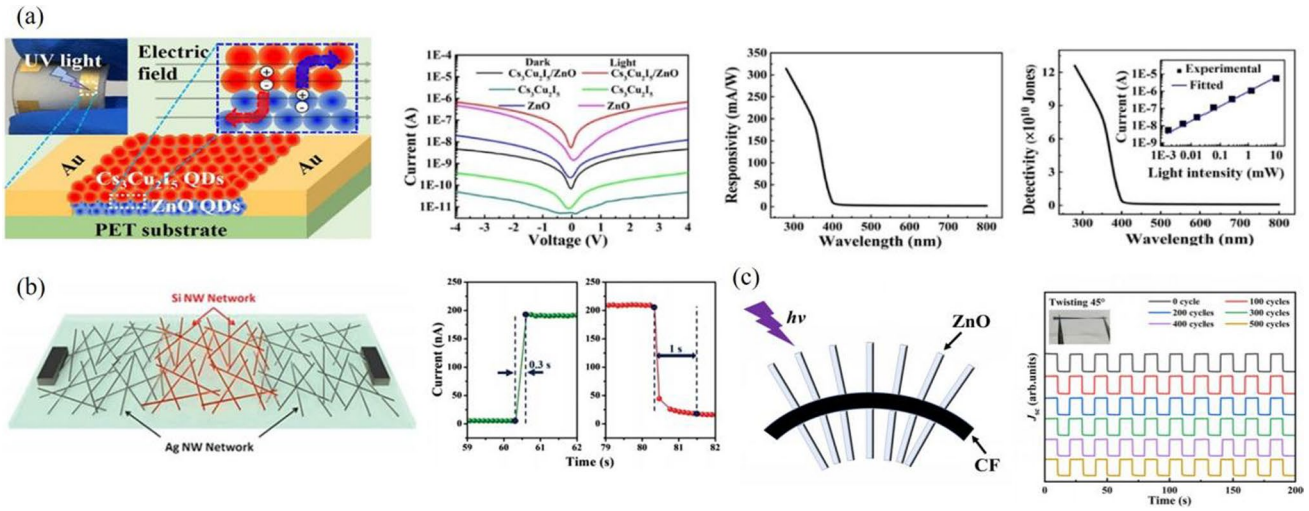

Fig. 2 **a** Schematic diagram of $Cs_3Cu_2I_5$/ZnO heterostructure PDs and corresponding electrical performance, responsivity, and detectivity [33], **b** schematic diagram of Si-nanowire-based PDs and corresponding response and recovery time [15], **c** schematic diagram of the flexible ZnO@Carbon fibers PDs and corresponding stability under different bending cycles [34]

2.4 Response/recovery time

Response time is the time elapsed by the detector from 10 to 90% of its saturated photocurrent when the light is turned on. Recovery time is the time required for the photocurrent to reduce from 90 to 10%. They can be divided into fast and slow response/recovery time. The fast response/recovery time is mainly attributed to the rapid valence band-conducting band transfer or recombination that occurs when light is activated (inactivated), while the slow response/recovery time is due to the oxygen vacancies, the carriers will be released (trapped).

2.5 Quantum efficiency (EQE)

EQE is the other main performance indicators [31]:

$$EQE = R\frac{hc}{q\lambda} \tag{3}$$

Under ultraviolet radiation, electron–hole pairs will be generated. Then, electrons are collected through separation and recombination of electron hole pairs inside the materials, and the ratio of the extracted free carriers to the incident photons is called EQE.

2.6 Detectability (D)

Detectability (D) is mainly used to describe the ability to detect weak light of device [32].

$$D = \frac{RS^{1/2}}{\left(2qI_{dark}\right)^{1/2}} \tag{4}$$

where, R denotes the responsivity, S denotes the effective irradiation area and $\left(2qI_{dark}\right)^{1/2}$ denotes the noise equivalent power.

2.7 Mechanical flexibility

Mechanical flexibility is also one of the main properties of electronic products. Generally, the time dependence of current without and with strain will be tested, and the changes in photocurrent before and after bending strain will be compared.

3 The structures of UV PDs

The structures of PDs are divided into vacuum type and solid-state type. The vacuum UV PDs are based on photomultiplier tubes and its derived imaging equipment, which is difficult to meet the requirements of weightlessness, integration and miniaturization. However, the solid-state type UV PDs are based on semiconductor materials, which is suitable for fabricating practical PDs. They can be classified into photoconductive and photovoltaic type according to operating principle. The photovoltaic type is the most used structure nowadays including Schottky [35], metal–semiconductor-metal (MSM) [36], p–n junction [37] and PECC type, as shown in Fig. 3. Besides, high-resistance intrinsic semiconductor layer is inserted between p–n junction to form p-i-n UV PDs, and the interface layer can prevent the recombination of electron hole pairs, improving the performance of the device.

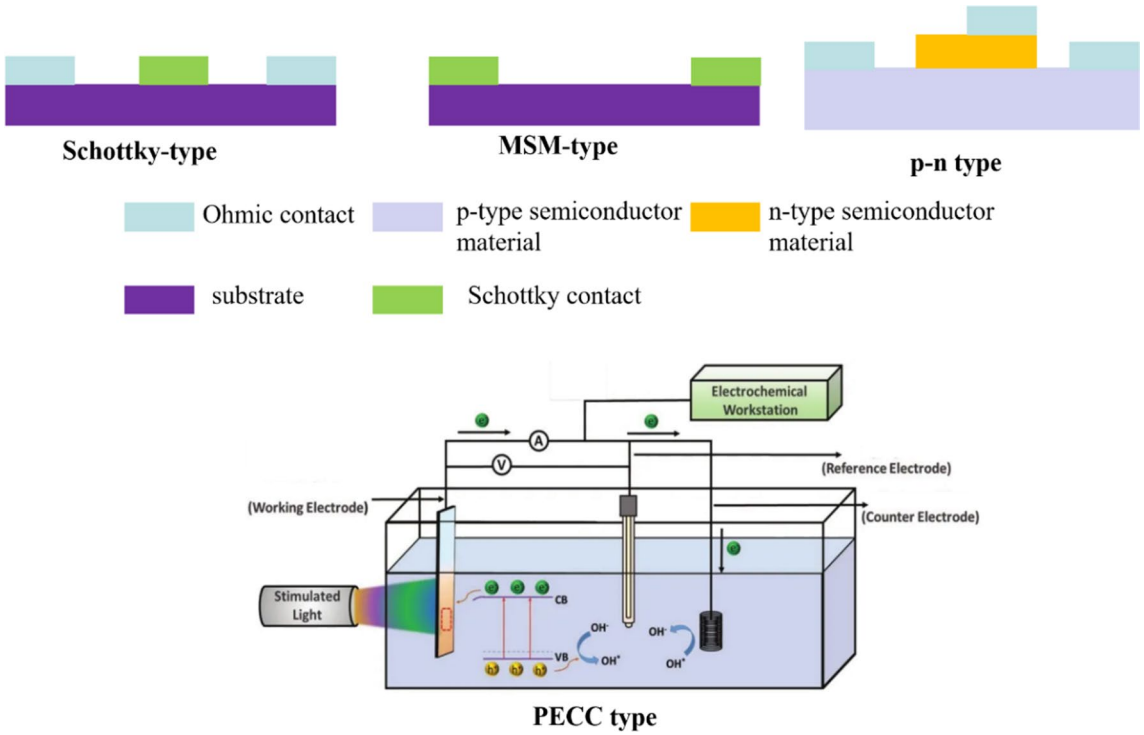

Fig. 3 Schematic diagrams of various photovoltaic solid-state UV PDs

3.1 Schottky type

Schottky-type structures require one electrode with Schottky contact and another with Ohmic contact. Generally, Au, Ag, Al and other metals are acted as the positive electrode, n-type semiconductor materials as the negative electrode. ZnO nanorods based flexible UV PDs with Cu nanowire electrode are fabricated [38]. Firstly, the Cu nanowire network electrode has a better transmittance, which is favorable for the UV radiation to reach directly below the electrode, and it has an appropriate square resistance and photoelectric stability, which is utilized to prepare UV PDs with better sensing effect. Secondly, the large specific surface area of ZnO nanorods facilitates efficient adsorption and desorption of oxygen molecules. In addition, the Schottky barriers generated by the formation of Schottky contacts between Cu and ZnO will help the separation of the photogenerated carriers generated under the light conditions, resulting in a strong detection capability of the device for UV light. Schottky contact is formed between Cu and ZnO, which enhances the photocarriers separation. Zhang et al. [39] synthesized Ag nanowire@ZnO nanorod composites based UV PDs with Au electrodes, as shown in Fig. 4a. The UV PD based on flexible and transparent Ag nanowire@ZnO nanorods exhibits high sensitivity and response speed under UV radiation due to the large depletion layer generated, the Schottky barrier between ZnO nanorods and Ag nanowires.

Duan et al. [35] fabricated graphene/ZnO:Al nanorod-array-film structure UV PDs, as is plotted in Fig. 4b. The corresponding energy band diagram is discussed. The Schottky contact show high sensitivity and fast photoresponse, and regulates the generation, transport and separation of carriers, resulting in a better rectification of the device [40]. Li et al. [41] proposed triboelectric voltage to reduce the Schottky barrier height of ZnO/Ag UV sensor, which validates the claim that electric fields can affect the behavior of charges on metal and semiconductor contacts (Schottky and ohmic contacts), and that the electric field generated by the friction electric technique lowers the Schottky barrier to enhance the photocurrent and responsivity of the UV PD, which will open up possibility for high sensitive self-powered UV sensing systems in the future.

Schottky contact between metals and semiconductor will inhibit photo-generated carrier recombination and can enhance absorption of UV radiation. The responsivity is greatly improved, and the dark current is smaller. Schematic diagram of Schottky barrier is shown in Fig. 5. The Fermi-levels are not equal between mental and semiconductor materials at first, the carriers will redistribute until the Fermi energy levels are equal when in contact with each other. The energy band bending will be occurred and the Schottky barrier will be formed [38]. When UV light irradiation, the photo-generated carrier are separated by the built-in electric field, and the directional movement of electron can form an

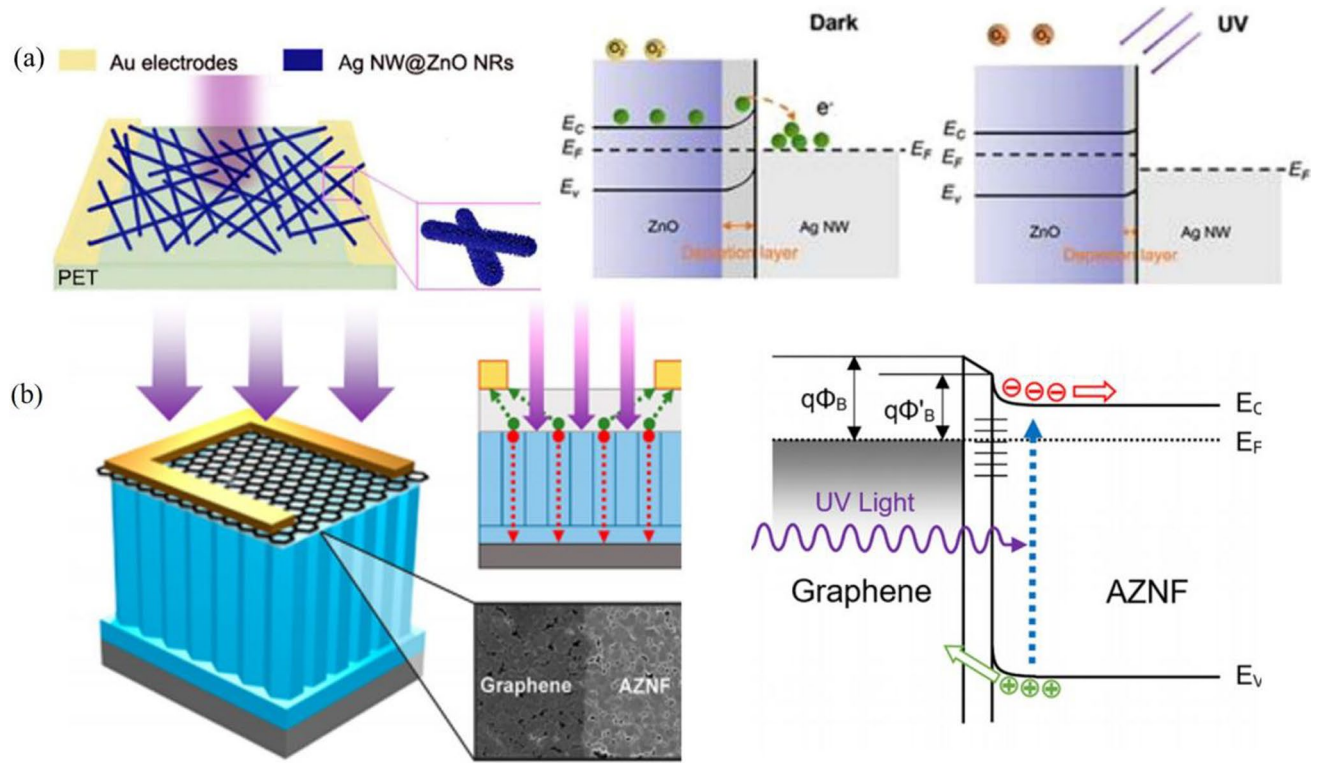

Fig. 4 Schematic diagram and energy band diagram of **a** Ag nanowire @ZnO nanorod PDs [39] and **b** graphene/ZnO:Al nanorod-array-film structure Schottky PDs [35]

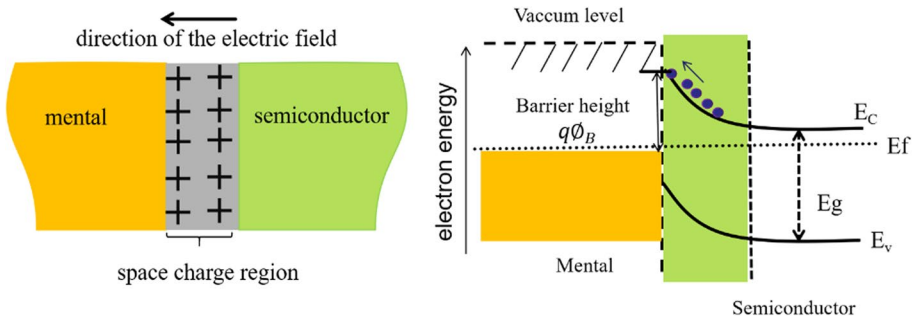

Fig. 5 Schematic diagram of Schottky barrier

electric photocurrent. The UV radiation can be determined by measuring the current value.

3.2 Metal–semiconductor-metal (MSM) type

MSM-type has become a popular PDs architecture due to large active area, fast response and easy production [18, 42]. It has two interconnected back-to-back Schottky junctions [43]. The MSM structure allows for both lateral and vertical carrier collection, making the collection of photogenerated carriers is more efficient, which greatly improves the responsiveness of the detectors. Schematic illustration of MSM-type structures is presented in Fig. 6, including one-dimensional parallel arrangement, one-dimensional vertical arrangement and sandwich structures [24].

Based on one-dimensional parallel arrays, the arrangement of nanomaterials is altered to form a one-dimensional vertical array structure. The responsiveness of such structural devices to light is determined by the density of the forked electrodes and the applied voltage, and their high performance mainly depends on the patterning of the electrodes and high external voltage. In addition, the sandwich structure is mainly in the form of top electrode/photosensitive micro-nanomaterials/bottom electrode. When it is used as an optoelectronic device, the light absorption capacity needs to be considered, so transparent electrode materials are usually used as the top electrode. Common transparent

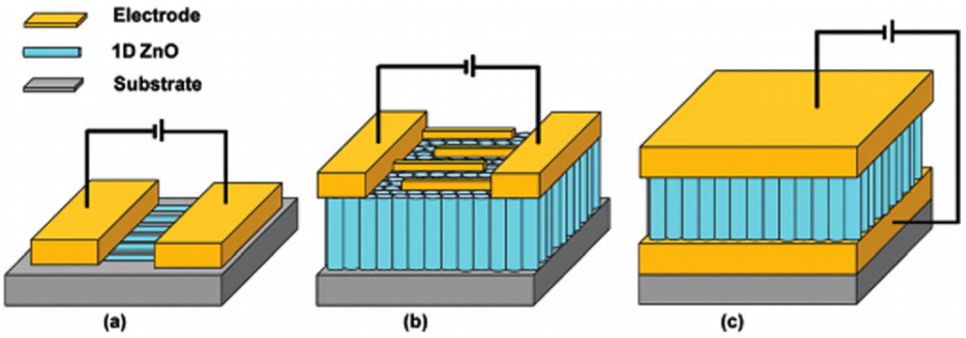

Fig. 6 Schematic diagram of different MSM UV PDs: **a** one-dimensional parallel array structures, **b** one-dimensional vertical array structure, **c** one-dimensional sandwich vertical structure [24]

electrode materials include Aluminium-doped Zinc Oxide, Indium tin oxide (ITO), and F-doped Tin Oxide, etc. Depositing transparent electrodes on transparent substrates using magnetron sputtering is the main strategy to improve the performance of UV PD.

Researchers have also attempted to modulate the performance of MSM-type devices through elemental doping (Fig. 7). Hunashimarad et al. [44] prepared MSM-type UV PDs using Ca-doped ZnO thin film as the active material. Compared with pure ZnO material, it has stronger absorption of UV light, higher response rate of 3.05 A/W under 365 nm UV irradiation and shorter response and recovery times of 15 s and 26 s, respectively. PDs with MSM structures generally exhibit the advantages of ultralow dark current, large photosensitive area and high responsivity. The UV detector of MSM structure usually has a large dark current, which mainly originates from the emission current of hot electrons or holes at the Schottky barrier as well as the tunnel current. In order to avoid the effect, certain measures are usually taken, including adding insulating layers, designing asymmetric electrodes, and increasing the height of the barrier so as to reduce the generation of the dark current. Fathima et al. [45] designed Sb doped ZnO based MSM-type UV PDs with Al interdigital electrodes. The results show that the photocurrent increases with increasing responsivity as the finger gap size decreases, and the sensitivity and efficiency of the device increases with decreasing electrode spacing. Previous literature also reported that the devices with asymmetric electrode have fewer defects, higher light-to-dark current ratios and improved performance compared to that of symmetric electrode.

3.3 p–n junction type

Simple wide-bandgap semiconductor materials have a large number of surface defects, which can cause photo-generated carrier recombination, so p–n junction is constructed to overcome these drawbacks [46]. The p–n junction is

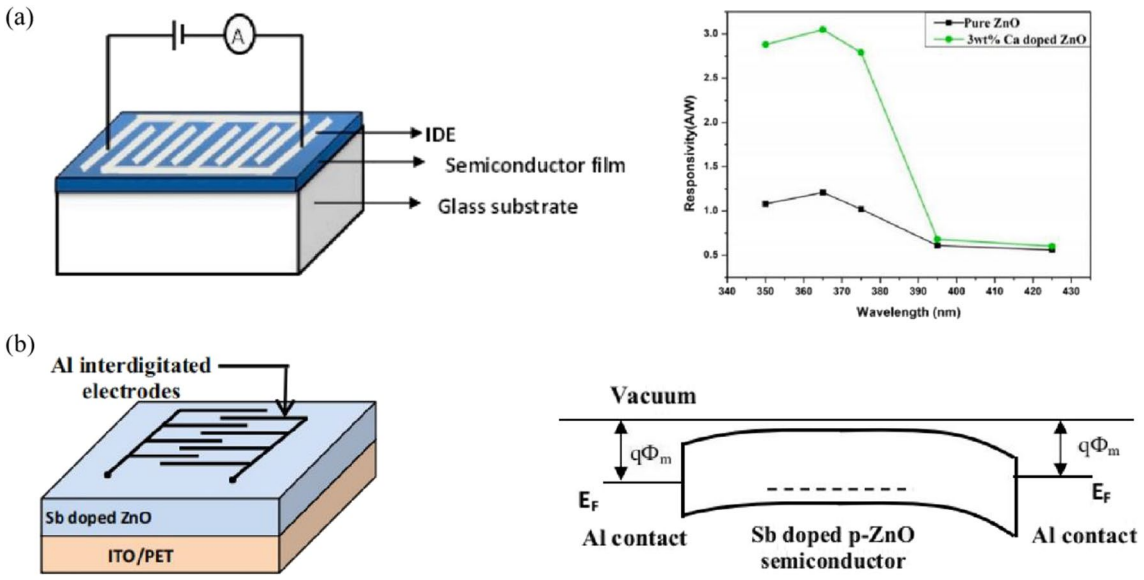

Fig. 7 **a** Schematic representation and spectral response of ZnO:Ca MSM Photodetector [44], **b** schematic illustration and Energy band diagram of Sb doped ZnO based Interdigitated UV PDs [45]

composed of p-type and n-type semiconductor, which is utilized promote the transport of charge carriers due to the unique arrangement of energy levels [47]. It can be divided into heterojunction and homo-junction.

3.3.1 Heterojunction

The structure formed by two semiconductor materials with different band gaps in contact with each other is called a heterojunction. Heterojunctions can be classified into p–n, p–p and n–n structures. However, for the composition of heterojunctions, it is usually required that the thermal expansion coefficients, crystal structure, and other properties between these two materials are similar. Based on quantum effect and high carrier mobility, it can be used as light-emitting devices, semiconductor laser diodes and solar cells, etc. The hierarchical arrangement of appropriate interfacial energy levels of the heterojunction structure can effectively promote the separation of photo-generated carriers and improve the responsiveness of the prepared devices. Li et al. prepared self-powered flexible transparent UV PDs with p-CuO/n-ZnO heterojunction [48], as is shown in Fig. 8a. The device exhibits fast rise and decay time, ultrahigh on/off ratio of 392 and after several times bending cycles, it still shows excellent mechanical stability.

More novel materials are used to construct heterojunctions. Amorphous semiconductor oxide materials have also been used in the design of electronic devices due to their low synthesis temperature and simple preparation. They include common low molecular amorphous materials, traditional oxide and non-oxide glasses and amorphous polymers. Figure 8b depicted constructed UV PDs based on CuI/α-ZTO heterojunction [13]. The detector can be self-powered with an on–off ratio of over 10^4 and has a fast response time of 2.36 ms and a recovery time of 1.49 ms, which also has good application potential at low temperature. Wang et al. [49] fabricated UV PDs based on n-ZnO/p-$SrCoO_x$ heterojunctions on a flexible polyimide-based substrate, as is shown in Fig. 8c. Due to the difference in Fermi energy levels and charge concentrations of the two materials, a built-in electric field is formed at the interface. Once irradiated with UV light, the electron–hole pairs in the ZnO films will be photo-excited and the built-in field rapidly separates them into opposite directions, resulting in a large photocurrent and fast response.

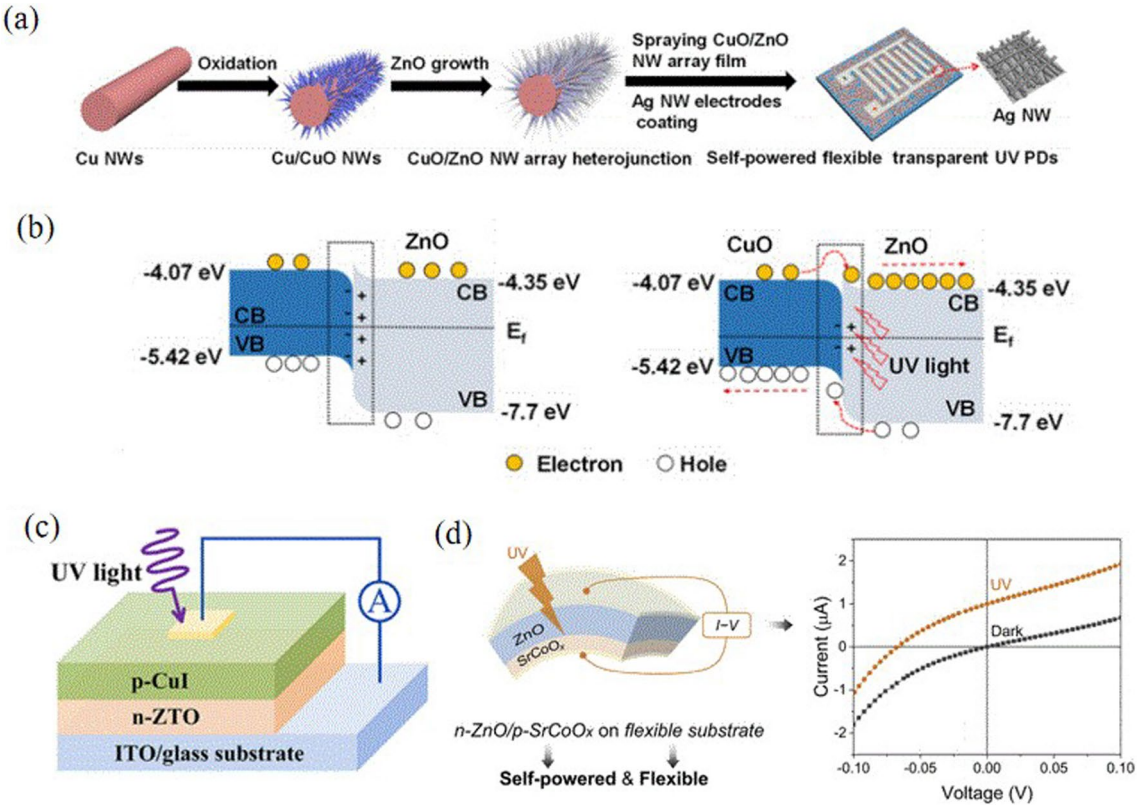

Fig. 8 **a** Preparation process for CuO/ZnO heterojunction UV PDs, **b** schematic diagram of the arrangement of energy bands of CuO/ZnO heterojunction [48], **c** Schematic diagram of CuI/ZTO heterojunction UV PDs [13], **d** schematic structure of ZnO/$SrCoO_x$ heterojunction flexible UV PDs, and corresponding electrical performance [49]

3.3.2 Homojunction

The homojunction is a structure composed of homogeneous semiconductor materials with the same of conductive type, which also includes p–n junction, p-p junction and n–n junction. It has a continuously curved energy band structure with high carrier mobility and low compounding rate. High quality p-type doping of ZnO, for the reason that it still exists obstacles in the construction of homojunctions. The preparation of p-type ZnO by doping group I or V elements has been widely used, these elements mainly act as metal catalysts. Chen et al.[50] assembled two independent ZnO nanorods into a face-to-face homojunction structure. The device has a strong absorption ability for UV light due to large specific surface area of ZnO nanorods. It can also be self-powered due to the presence of Schottky barriers. Under UV irradiation of 3.06 $\mu W \bullet cm^{-2}$, it has a responsivity of 2.45 $mA \bullet W^{-1}$ and a switching current ratio of 6.6×10^5. In order to construct homogeneous p-n junctions, doping is often used to change the conductivity of the materials. Wang et al. [51] prepared Sb doped ZnO/ZnO p-n homojunction based self-powered UV PDs. A robotic arm is used to contact ZnO and Sb-ZnO, as is shown in Fig. 9a. This is an efficient and precise micro-nano assembly technology, which can assemble two different bandgap materials together successfully to form a homojunction, and can achieve a response to a wider band of ultraviolet radiation. However, metal dopants can cause deep defects in the material that affect the overall device performance, so MgO dielectric layer is used to modify the p-ZnO:Sb/n-ZnO homojunction interface [52], and the optimized PDs show enhanced UV detection capabilities(Fig. 9b).

3.4 Photoelectrochemical (PECC) type

PECC-type structure is a unique sandwich architecture that encapsulates the electrolyte between photo-anode and cathode. The working electrode is generally composed of semiconductor material grown on transparent conductive oxide (ITO and F-doped Tin Oxide) glass, and the counter electrode is generally a platinum electrode. This structure has received widespread attention due to its fast response to ultraviolet radiation, simple production process, high stability and ability to realize comprehensive detection of ultraviolet light [34]. Figure 10a presented PECC-type UV PDs based on $KNbO_3$/ZnO heterojunction [53]. Under UV irradiation, the anode absorbs photon energy, the photo-generated electrons are transitioned and finally are collected by the Pt electrode to realize ultraviolet light monitoring. However, using transparent conductive glass as a substrate will limit flexibility and its applications. Zhang et al. [34] prepared flexible PECC-type UV PDs based on ZnO@Carbon fibers, as is shown in Fig. 10b. It is developed by growing ZnO nanowires using the hydrothermal method on CFs, the device outputs a stabilized photocurrent of 185 $\mu A \bullet cm^{-2}$, as well as repeatability and ultra-fast response recovery time, which opens up new avenues for the development of novel flexible UV detectors.

Performance of different structural types of photodetectors is compared, as is shown in Table 1. We can see that the response/recovery time of the device based on the heterojunction structure is three orders of magnitude better than that of the other structures, and the responsiveness and sensitivity are also significantly improved.

4 Ultraviolet detector materials

Third-generation semiconductors are often used in PDs, which is mostly metal oxide semiconductor materials with wide bandgap more than 2.3 eV depicted in Table 2 [54, 55]. Many useful properties including low dielectric constant, high breakdown field, good thermal conductivity, high electron saturation rate and radiation resistance are sumarized in Table 2, satisfying the preparation conditions for UV PDs [56].

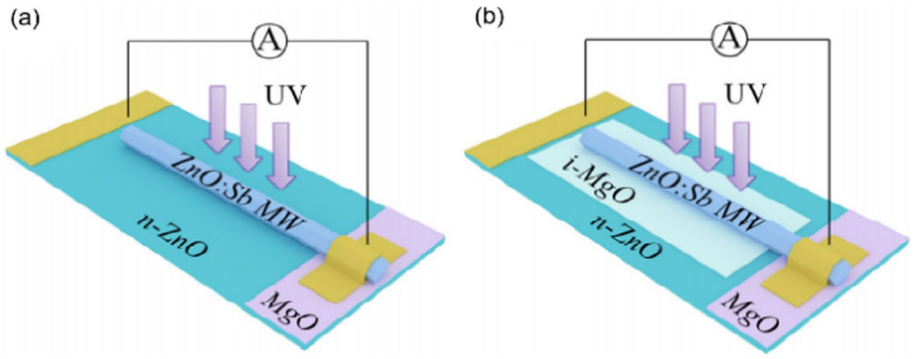

Fig. 9 Schematic architecture of (a) p-ZnO:Sb/n-ZnO homojunction and (b) p-ZnO:Sb /i-MgO/n-ZnO homojunction PDs under UV radiation [51]

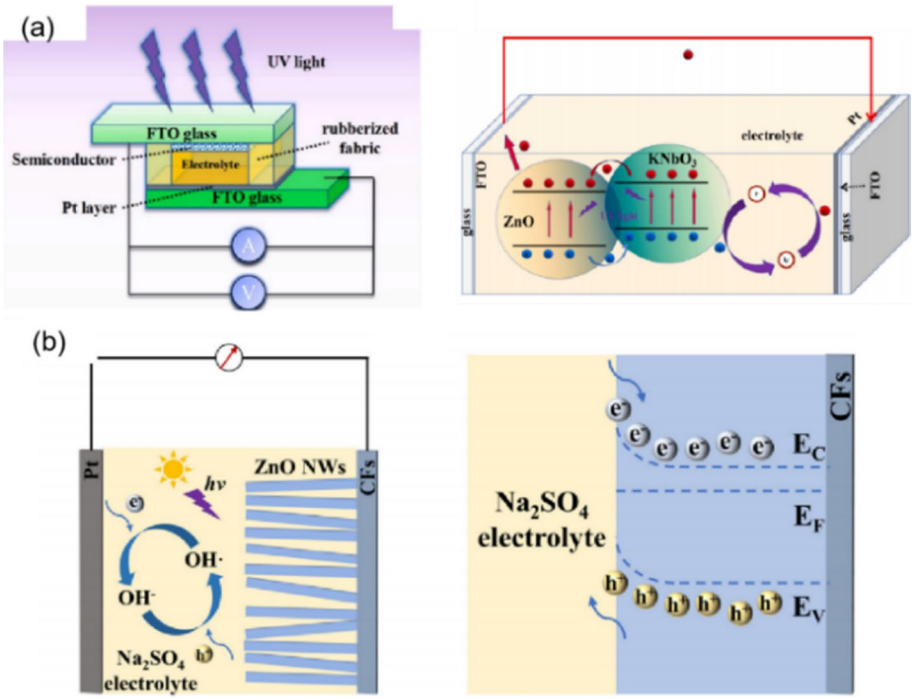

Fig. 10 **a** Schematic diagram and working mechanism of the PECC UV PDs based on the $KNbO_3$/ZnO heterojunction [53], **b** schematic and energy band diagram of the ZnO@ Carbon fibers PECC-type UV PDs [34]

Table 1 Performance comparison of different structural types of photodetectors

PDs structures	Responsivity	On–off ratio	Response time	References
Schottky type				
Graphene/ZnO:Al	0.04 A/W	–	37/330 μs	[35]
Ag NW@ZnO NRs	–	23.2	0.7/1.9 ms	[39]
Graphene/GaN	10^{-5} A/W	–	221/546 μs	[40]
MSM type				
$Zr_{0.1}Ti_{0.9}O_2$/Au	180 A/W	–	–	[43]
ZnO: Ca/Al	3.797 A/W	–	–	[44]
p-n type				
Ga_2O_3/Cu_2O	36.2 mA/W	–	7.95/8.39 ms	[1]
CuI/*a*-ZTO	19.1 mA/W	137	26.9/13.6 ms	[13]
CuO/ZnO	1.68 mA/W	392	16/17 ms	[48]
PECC type				
ZnO@CFs	185 uA/cm^2	–	0.17/0.12 s	[34]
$KNbO_3$/ZnO	57 mA/W	8/11	8/11 ms	[53]

Table 2 Some performance parameters of relevant ultraviolet detector materials

Semiconductor material	SiC	Diamond	GaN	ZnO
Band gap type	indirect	indirect	direct	direct
Band gap (eV)	2.994	5.5	3.36	3.37
Melting point (°C)	2830	4000	1700	1975
Electron mobility ($cm^2 \bullet V^{-1} \bullet s^{-1}$)	8000	1000	2200	900

4.1 Semiconductor oxide

Most of research on PDs in recent years has been based on wide bandgap metal oxide semiconductor materials, such as ZnO, Ga_2O_3, TiO_2 and others. These semiconductor materials will be introduced respectively.

4.1.1 ZnO

ZnO has strong absorption of UV owing to wide band gap of 3.37 eV and high exciton binding energy, and also has high carrier mobility and strong thermal stability, which makes it an ideal material for PDs [24, 33, 40]. The morphologies of nanomaterial mainly includes nanorods [57], nanowires [58], nanofilms [59] and nanotubes [60] etc. The nanorod structure has become a promising structure for the fabrication of PDs due to its high aspect ratio, better light reflection and absorption effects. Salah et al. [61] prepared UV PDs by depositing ZnO nanorods on Poly (propylene carbonate). The corresponding mechanism can be described by Fig. 11a. When UV is turned off, semiconductor surface will form a low-conductivity depletion layer. Electrons in valence band transition to conduction band and the holes move to the semiconductor surface, resulting in the formation of photocurrent [61]. However, the defects of ZnO limit its response and recovery time, ZnO-based hybrid materials can effectively solve this problem. Moreover, the absorbance of incident light and property of PDs can be increased by surface modification, metal adsorption and dopant.

PEG is added into ZnO nanoparticles to improve the ductility of the film and its mechanical stability when subjected to strain [62], as is shown in Fig. 11b. By coating the ZnO/PEG composite on paper, the flexible PDs show a high responsivity and a large specific detectivity. Notably, a giant on-off ratio of up to 1.99×10^5 has been achieved by suppression of dark current. PEI [63] has been added into hydrothermal solution as the growth additive to obtain the ultra-long ZnO nanorods and in turns improves the performance of PDs. In order to suppress the surface defects and improve the photoelectric properties of ZnO materials, metal doping is usually selected. The Group V elements are generally used for p-type doping in ZnO. Mondal et al. [64] doped P into ZnO films to tune its point defects. Due to acceptor-donor compensation provides the advantage of an ultralow dark current, P doped ZnO films show a high responsivity and detectivity compared to pristine ZnO. Transition metal elements (Mn) [57] and Ga [61] is also commonly used for doping to optimize the properties of ZnO nanomaterials.

4.1.2 Ga_2O_3

The wavelength less than 280 nm of radiation is called solar-blind UV, and mostly is absorbed by the ozone layer during its propagation to the ground. With the rapidly increasing demand for solar-blind UV PDs on military and life, it has become a research hotspot. Ga_2O_3 has significant deep UV absorption properties, which is a quasi-direct wide-bandgap oxide semiconductor with band gap of 4.5–5.3 eV and corresponding cut-off wavelength of 280 nm. Excellent radiation hardness, high thermal and chemical stability, inexpensive, low noise and high sensitivity, making it a desired material for solar-blind PDs [65–72]. The most commonly chosen structure for building Ga_2O_3-based solar-blind UV PDs is MSM-type structures. As is shown in Fig. 12a, a novel fully transparent MSM solar-blind UV PDs with ITO digital inter-electrode based on Ga_2O_3 film is designed [73]. When β-Ga_2O_3 is in contact with two embedded ITO electrodes on both sides, an electric field with uniform distribution and high strength is formed between them, and with the high crystallinity and good crystallization quality of the thin film prepared, the overall performance of the device is enhanced. β-Ga_2O_3 is the most stable among various Ga_2O_3 single crystal [68, 74]. However, β-Ga_2O_3 crystalline materials should be annealed at an ultrahigh temperature to realize high performance, which further increases the cost and complexity [75]. In addition, high temperatures are not suitable for the preparation of flexible detectors. Amorphous Ga_2O_3 (a-Ga_2O_3) has high compatibility with various substrates and simple preparation at low temperature. Zhang et al. [69] developed a low temperature process for the

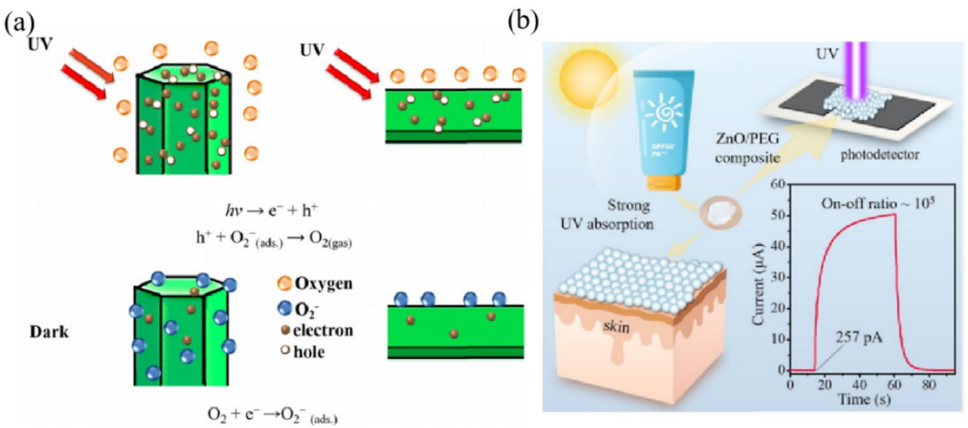

Fig. 11 **a** Schematic illustration of the mechanism of ZnO nanorods UV PDs [61], **b** schematic diagram, response times and the on–off ratio of the UV PDs based on the ZnO/PEG composite film and carbon electrodes [62]

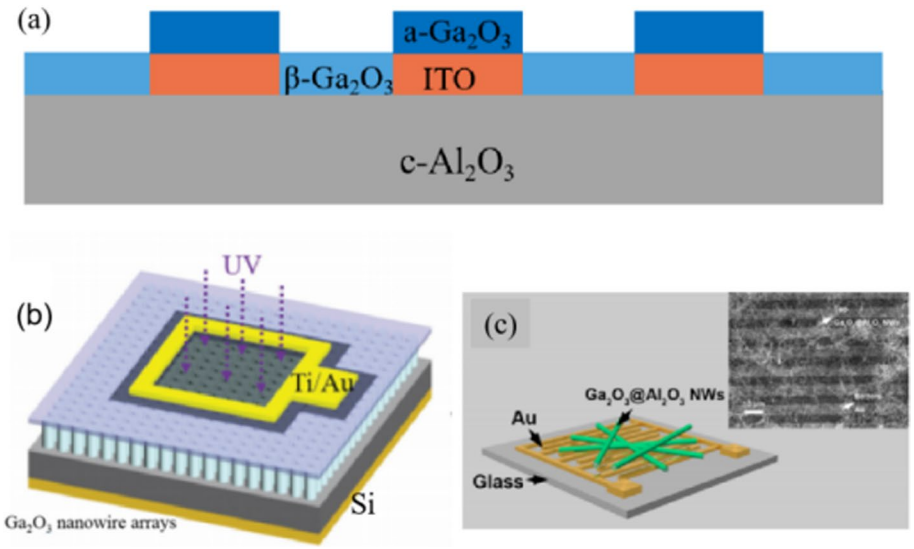

Fig. 12 Schematic illustration of UV PDs based on Ga_2O_3: **a** Transparent MSM solar-blind UV PDs with ITO digital inter-electrode based on Ga_2O_3 films on c-Al_2O_3 substrate [73], **b** dual-band ZnO/Au/Ga_2O_3 sandwich structure UV PDs [71], **c** Ga_2O_3@Al_2O_3 core–shell nanowires with the Au interdigital electrode solar-blind UV PDs [[76]]

preparation a-Ga_2O_3 nanosheet and fabricated a flexible self-powered PDs, which exhibits excellent photodetection behaviors. All results promote the development of Ga_2O_3 based optoelectronics. He et al. [71] proposed a solar-blind UV PDs based on the graphene/vertical Ga_2O_3 heterojunction plotted in Fig. 12b. The device exhibits fast responsivity and high rejection ratio, which is attributed to large specific surface area of nanowire arrays and heterojunction structure. Jiang et al. [76] fabricated Ga_2O_3@Al_2O_3 core–shell nanowires based solar-blind UV PD plotted in Fig. 12c. Al_2O_3 layer plays a passivating effect and suppresses the defects. When Au electrode contact with Ga_2O_3 nanowires, Schottky junction is formed and facilitates the separation and transport of photogenerated carriers.

4.1.3 TiO_2

TiO_2 is also a wide bandgap semiconductor material, which is chemically inert nature, prominent biocompatibility and nontoxicity [12, 76–79]. TiO_2 can be obtained as anatase polycrystals (500 °C) and rutile polycrystals (800–1000 °C) depending on the annealing temperature [78]. Due to strong absorption of UV and also as the main ingredient in sunscreen, TiO_2 is widely used in fabricating PDs [[80]]. However, the high-temperature preparation leads to a complex fabrication process and high experimental cost, which is an obstacle to large-scale production and application of the devices. Zhang et al. [22] fabricates UV PDs by spin-coating poly (9, 9-dihexylfluorene) on the TiO_2 array shown in Fig. 13a. Hybrid materials of inorganic semiconductor nanocrystals and conjugated organic molecules improve the performance of PDs. As is plotted in Fig. 13b, Tran et al. [81] prepared TiO_2 nanoparticles by a simple sol–gel method and constructed a solar-blind UV PDs. In order to reduce the surface defects and enhance the light absorption, acetic acid is introduced to modify the material during the experiment, which results in a significant reduction of oxygen vacancies and defects in the TiO_2 material. Moreover, it is also concluded that the band gap is increased and the device performance is enhanced.

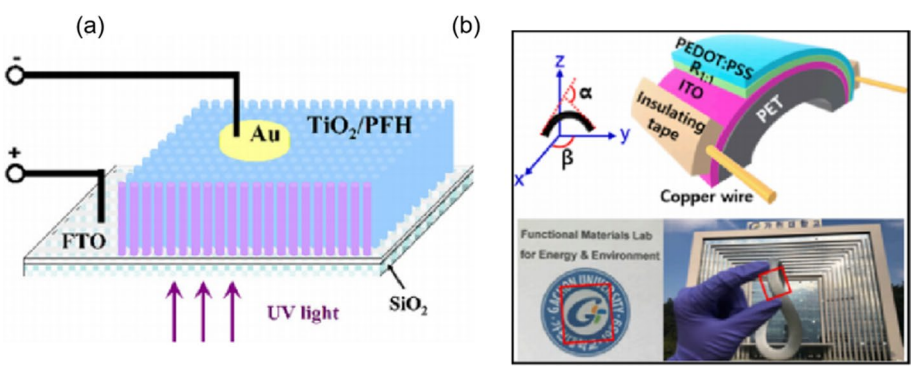

Fig. 13 Schematic illustration of UV PDs based on TiO_2 [22, 81]

4.2 Alloy materials

Alloy material can achieve the detection of solar-blind ultraviolet due to adjustable band gap, and the fabrication of UV detectors based on alloy materials is mainly realized by bandgap modulation. The alloy materials that have been reported to be used in the fabrication of solar-blind UV detectors include ternary alloys BeZnO, MgZnO and AlSnO, etc. [82–84]. Xu et al. [85] realized the growth of AlSnO thin films with a continuously adjustable bandgap in the range of 4.40–5.43 eV by magnetron sputtering, and prepared a narrow-band solar-blind UV detector, which shows great advantages in solar-blind UV spectral selectivity and detectability. For the BeZnO ternary alloying material, due to the large lattice mismatch between ZnO and BeO, which prevents the formation of alloying materials, doping with a high concentration of Be can broaden the energy bands of the material and overcome the persistent photoconductivity effect. E et al. [86] modulated the band gap of the ternary alloy BeZnO in order to make the material capable of detecting solar-blind UV radiation. UV PDs are prepared on rigid and flexible substrates by doping a large amount of Be elements in ZnO to form amorphous BeZnO films and depositing Al electrodes on them, respectively. Since elemental doping leads to the reduction of defects, these experimentally constructed detectors all produce small dark currents with high sensitivity and response to UV light (Fig. 14). Amorphous materials are prepared by low-temperature process, which can prevent the film from non-crystallization or phase separation, and are compatible with flexible substrates, which provides a better idea for the realization of flexible day-blind ultraviolet PDs in the future.

4.3 Superlattice materials

Superlattice materials are grown from thin layers of materials with a lattice matching degree of tens of nanometers, with each layer having a thickness of less than 100 nm [87].This is a layered composite material with a specific form that is stacked alternately along the length of the nanowires. Superlattice nanowires, as active channel materials for PDs, facilitate the separation and collection of photogenerated carriers at the heterojunction interface, which can greatly improve the device performance [88, 89]. Superlattice nanowires with unique energy band structures can effectively separate and collect photocarriers, and thus become a worthy material to explore the properties of high-quality PDs. Li et al. [90] prepared InGaZnO superlattice nanowires by atmospheric pressure chemical vapor deposition. Along the axial direction of the nanowires, the $InGaO(ZnO)^{4+}$ and InO^{2-} layers are perfectly stacked alternately to form a periodic laminar structure. In this study, the researchers first observed the detectability of single NW devices for UV light and found that Ga concentration significantly affects the number of oxygen vacancies and oxygen molecules adsorbed on the

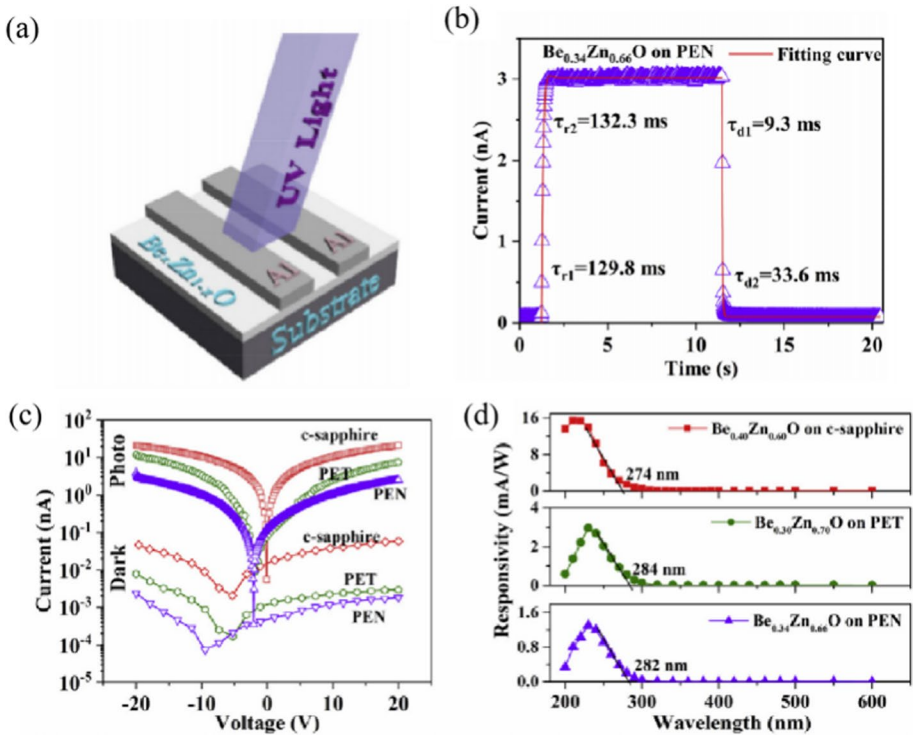

Fig. 14 **a** Schematic diagram of BeZnO PDs, **b** Response/recovery times of devices based on flexible polyethy- lenenaphthalate substrates, **e** I–V curves in the dark and under illumination, **f** Spectral responsivities of three devices [86]

NW surface. Based on the optimized $In_{1.8}Ga_{1.8}Zn_{2.4}O_7$, the single NW device exhibits an excellent responsivity of 1.95×10^5 A/W, an external quantum efficiency as high as 9.28×10^7%, and response and recovery times of 0.93 s and 0.2 s, respectively. Secondly, the researchers constructed fully transparent UV photodetectors based on superlattice NW arrays, which have superior performance to many high-performance transparent photodetectors. The results discussed above demonstrate the great potential of InGaZnO superlattice nanorods for next-generation advanced optoelectronic devices. This provides ideas for the design of flexible UV PDs based on superlattice structures. Lou et al. [91] successfully synthesized $InGaO_3(ZnO)$ superlattice nanowires by a simple vapor transport technique. Field effect transistors and UV detectors are prepared. The atomic ratio of In:Zn has a great influence on the performance of the devices. As prepared sensor has a strong sensing ability for UV light due to the spatial separation of photogenerated carriers at the interface, with a spectral responsivity of 5.3×10^4 A•W^{-1}, a high external quantum efficiency of 1.9×10^7, and a fast response speed of 0.3 s. In addition, the device has good mechanical stability after multiple bending strains and has the potential to become a flexible wearable device. (Fig. 15). $InGaO_3(ZnO)$ nanowires have great potential application in nanoscale optoelectronic devices.

4.4 Perovskite

Perovskite is an inorganic, non-metallic material that can be classified as layered, columnar and rock salt ordered chalcopyrite. Generally, it has the formula of ABX_3, where, A is a monovalent cation, B is a divalent metal cation, X denotes an anion, and it can be classified as oxide or halide chalcopyrite [92–94]. Perovskite have the advantages of high absorption coefficients, long-range equilibrium electrons, hole diffusion lengths and high carrier mobility [95, 96]. Novel organic–inorganic hybrid materials are used to prepare UV detectors due to their low cost, tunable bandgap, good spectral selectivity, and the fact that they can be prepared by simple solution processing [97]. Zhang et al. used a modified low-temperature (70 ℃) solution-processing method to obtain high-performance photoconductive devices based on $CsPbBr_3$ thin films, which has broadband spectral response from the solar-blind region to the visible light [[92]].

However, solution-treated perovskites show poor morphology and crystallinity. Therefore, Zhou et al. [97] prepared ITO/PET/SnO_2/$MAPbCl_3$/PTAA/Au flexible UV PDs using a solution-assisted halide exchange strategy to convert conventional solution-processed $MAPbBr_3$ films into homogeneous $MAPbCl_3$ films, as is plotted in Fig. 16a. This flexible detector can be used to develop wearable flexible UV wristbands for real-time monitoring of UV radiation. Recently, Al halide materials $CH_3NH_3PbCl_3$ has been investigated for UV detection. Therefore, Wu et al. [93] developed tandem photoelectric sensors based on perovskite/carbon nanotube hybrids, which can distinguish UV, visible and infrared spectra under different light intensities. In addition, 2D perovskite is focused in PDs field [98] due to ultrahigh resistivity, appropriate bandgap and increased stability. Han et al. chose PMA^+ as the interlayer ion for the preparation

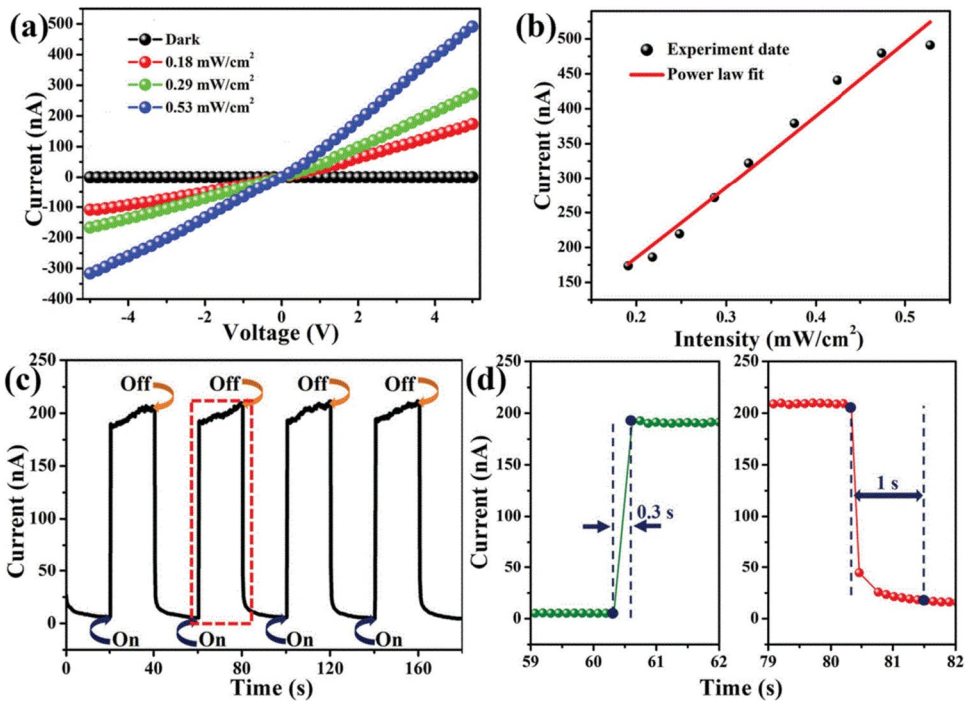

Fig. 15 **a** I–V curves under different UV power, **b** dependence of photocurrent on light intensity, **c** photo-response properties of the PDs, **d** response and recovery time [91]

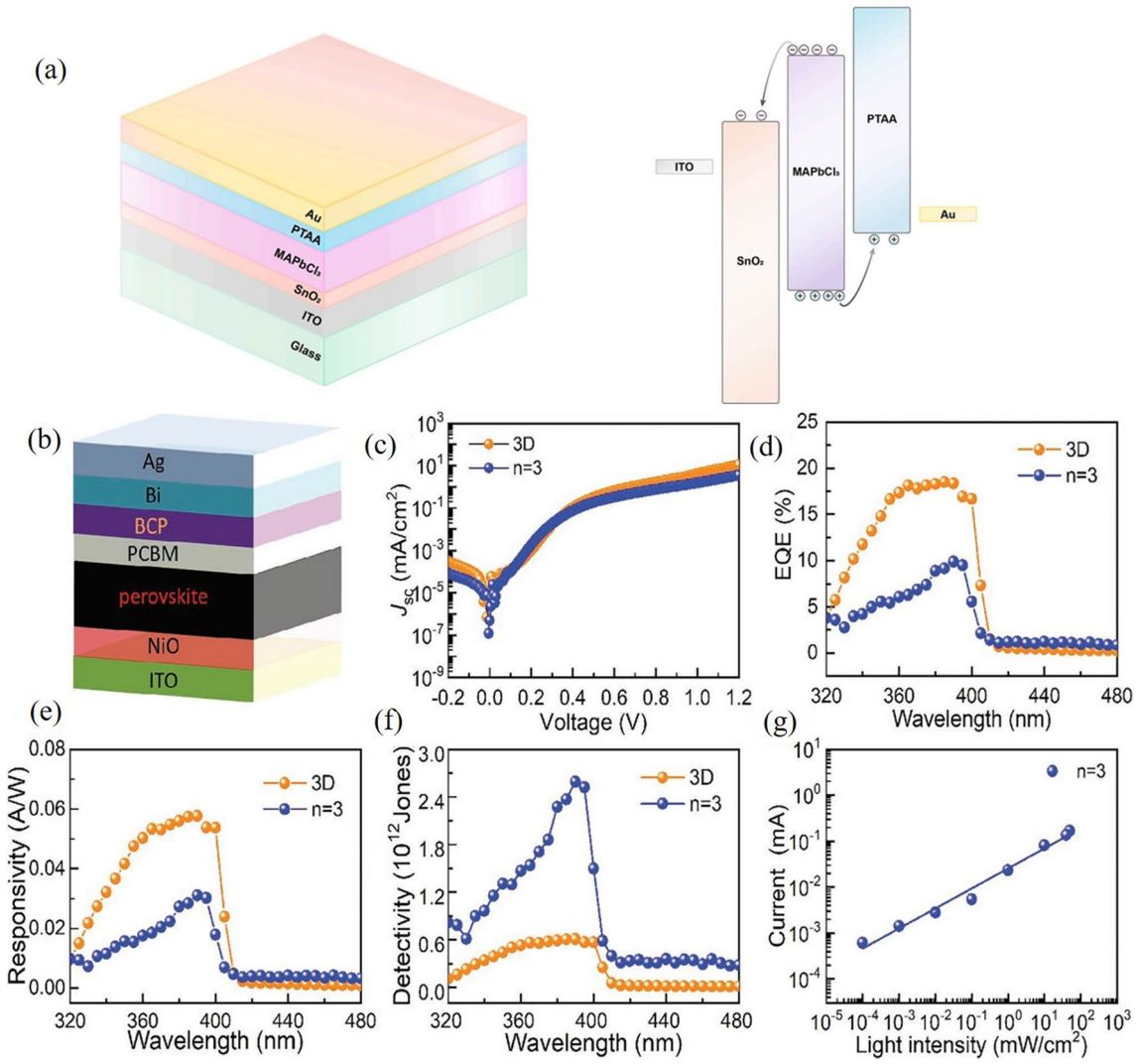

Fig. 16 **a** Schematic structure and energy band structure of ITO/PET/SnO_2/$MAPbCl_3$/PTAA/Au flexible UV PDs and **b–g** Schematic structure and corresponding performance testing of ITO/NiO/perovskite/PCBM/BCP/Bi/Ag UV PDs [97]

of 2D perovskite films, and prepared high-quality quasi-2D Ruddlesden-Popper chalcogenides [99]. This facilitates the reduction of the dark current of the device, as is plotted in Fig. 16b–g.

4.5 Other materials

4.5.1 Graphene

Graphene has high carrier mobility, large surface area, high electrical conductivity and effective current transport channels. It is often used as a transparent electrode based on its excellent transmittance to ultraviolet radiation [100]. As shown in Fig. 17a, graphene/GaN nanorod heterojunction UV PDs is prepared from top-down by combining dry and wet methods [101]. Schottky contact is formed between graphene and GaN nanorods to create a built-in electric field, and electrons flow into graphene to generate photocurrents due to low Fermi energy level. This structure has a fast photoresponse compared to metal electrode devices. Graphene quantum dots are also used to enhance device performance by enhancing the efficiency of photo-generated charge separation and transport [102]. Yin et al. [103] modified ZnO nanorods with graphene quantum dots, and the UV sensitivity of the device is increased. It can be explained that when the

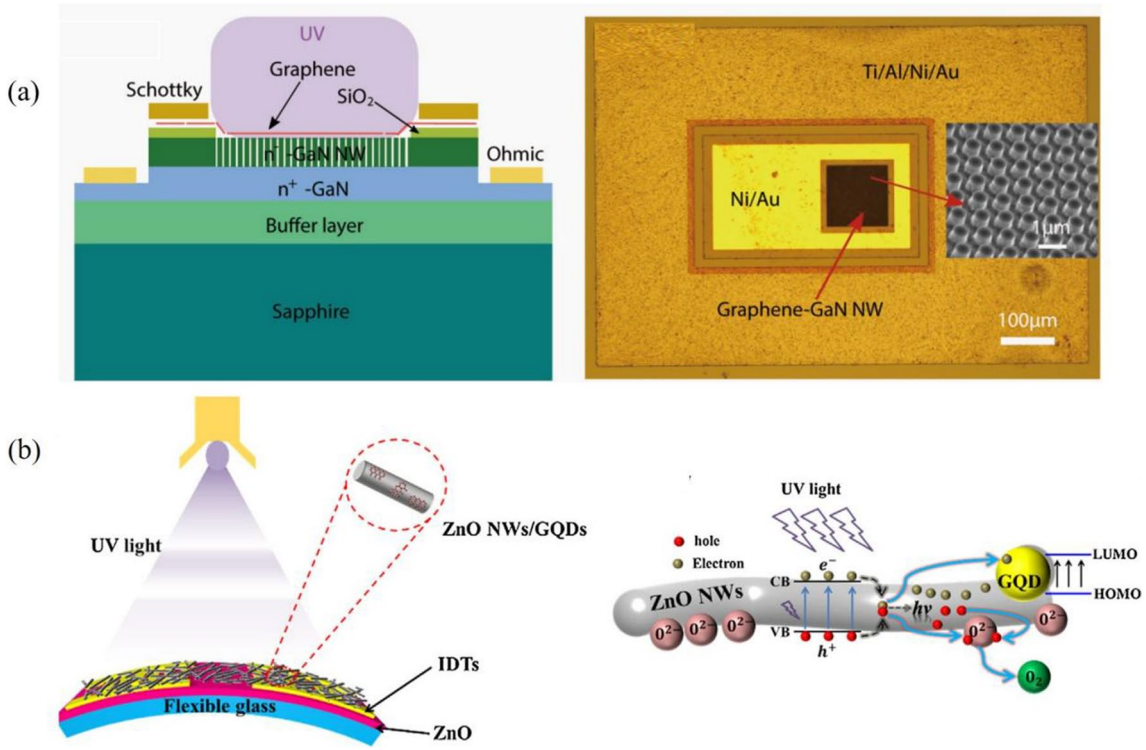

Fig. 17 **a** The cross-sectional structure and optical microscope image of the graphene-GaN heterojunction UV PDs [101], **b** schematic diagram and mechanism of GQDs@ZnO-nanowires nano-composites under ultraviolet conditions [103]

quantum dots are on the surface of the nanorods, a new channel is provide for photogenerated charge transport, which enables the efficient separation of photogenerated carriers, as is plotted in Fig. 17b.

4.5.2 ZnAl:LDH Nanosheets

The new generation of UV PDs tend to develop biodegradable, environmentally friendly material [104]. Layered double hydroxide (LDHs) are promising two-dimensional materials, alternative name is anionic clays and hydro fossil-like materials. It consists of a metal cation layer inserting anions and water molecules to fill the interlayer space. The formula is expressed as $[M_{1-x}^{2+}M_x^{3+}(OH)_2]^{x+}[Ax/n]^{n-}\cdot mH_2O$, where M^{2+} and M^{3+} are divalent and trivalent metal ions, respectively, A^{n-} denotes inorganic or organic anions, m is the number of water molecules in the interlayer, and x denotes the molar metal cation ratio, $x = M^{3+}/(M^{2+} + M^{3+})$.

The band gap can be obtained from absorption spectra of the ZnAl:LDH material. The Tauc formula expresses the relationship between the optical absorption coefficient and the photon energy: $(\alpha h\nu)^{1/n} = B\ (h\nu\text{-}E_g)$, where $h\nu$ is the photon energy, B is the proportionality constant, and E_g is the band gap energy. ZnAl:LDH is a direct-bandgap semiconductor and can be used as a preparation material for intrinsically visible blind UV PDs. LDHs can modulate properties by binding to a variety of metal cations and anions [105–109]. ZnAl:LDH is used to construct flexible UV detectors due to excellent UV absorption properties, low-temperature hydrothermal method, and high flexibility.

Thomas et al. [110] demonstrated environmentally friendly ZnAl-CO_3:LDH in high performance flexible UV PDs. Both spectral responsivity and detectivity are improved by passivating ZnAl:LDH Ns with PDMS. Jeon et al. [111] constructed flexible visible blind UV PDs based on vortex-structured 2D ZnAl layered double hydroxide (LDH) nanosheets. The devices exhibit photoresponse in the UV spectral range. In addition, the peak responsivity of the UV PD is 17 mA/W under 365 nm illumination. The increase in conductivity as well as photocurrent of the UV detector under UV irradiation mainly depends on the oxygen adsorption and desorption processes on the surface of the material. The surface reaction of LDHs is shown in Fig. 18d. In the absence of light, oxygen molecules capture free electrons adsorbed on the material surface, forming a low-conductivity depletion region. Energy band bending increases the amount of O_2 adsorption and there is a low current in the oxygen-rich environment. When UV light is irradiated, photogenerated carriers are produced, leading to an increase in

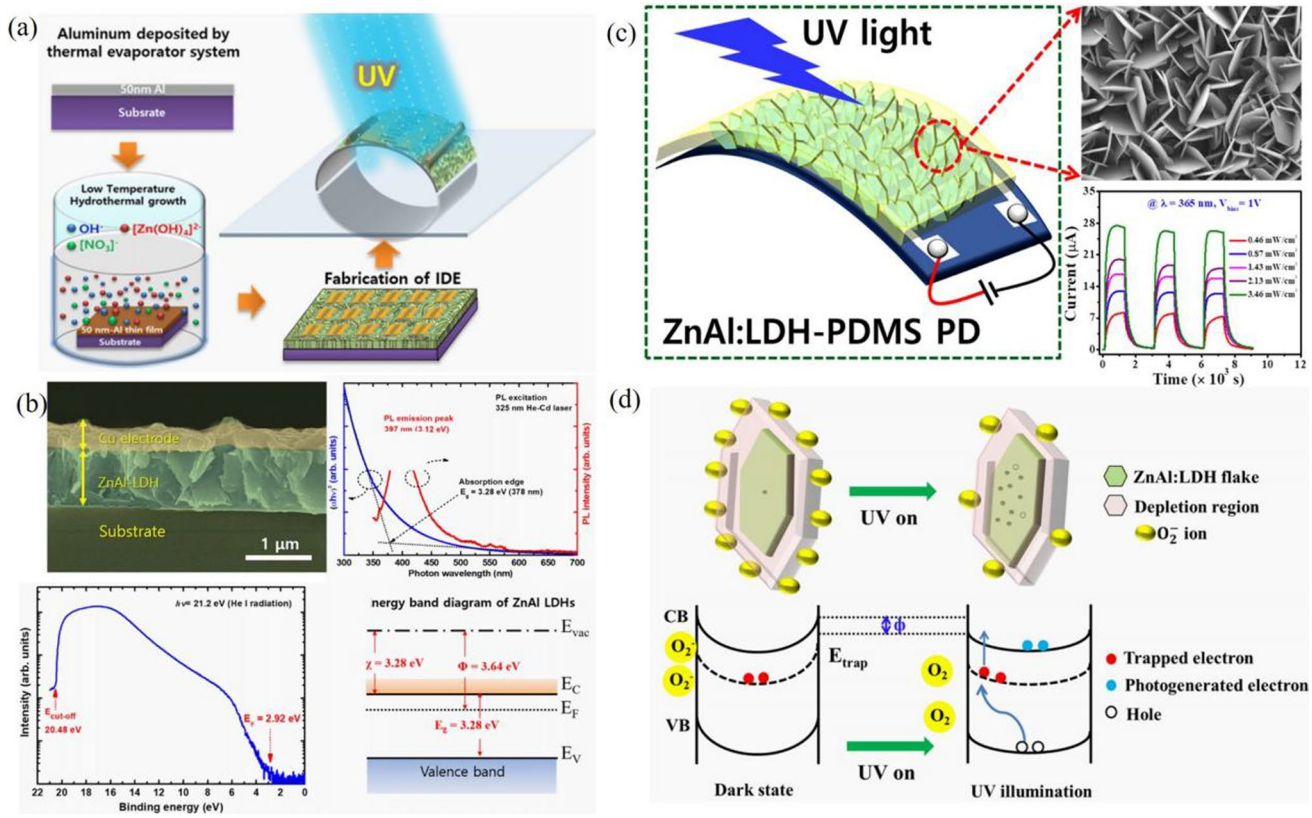

Fig. 18 **a**, **b** Schematic and Surface image of ZnAl-LDH scroll-based UV PDs. Variation in photocurrent with light wavelength. The inset is the energy band diagram [111], **c**, **d** schematic representation and related properties of ZnAl:LDH-PDMS PDs [110]

photocurrent. The flexible PD is more stable even after 1000 bending cycles, as is plotted in Fig. 18.

5 Performance

5.1 Piezoelectric effect

Interfacial engineering of semiconductor materials has been the focus of research efforts in related fields, and piezoelectric photoelectronic effects are commonly used in the preparation of PDs [112]. The coupling of piezoelectric effect and optical excitation produces a new effect to regulate the photogenerated carriers with the help of stress [113]. When the semiconductor material is subjected to external stretching, compression and other stresses, due to the generation of piezoelectric field, the interface structure and carrier transport, separation and recombination play a regulatory role in optimizing the performance of UV PDs, mainly manifested in the band offset and the change in the height of the potential barrier [112, 114].

Semiconductor materials with piezoelectric properties are ZnO, CdSe and other II-VI compounds and GaSb, InSb, AlN and other III-V compounds. Piezoelectric semiconductor materials with a non-centrosymmetric structure have a certain ionic nature, and in the absence of felt changes in external forces, their positive and negative ions are spatially overlapping. When feeling the externally applied strain, positive and negative ions will move to produce a certain distance, resulting in a dipole moment and electrode phenomenon, the upper and lower surfaces of the semiconductor material will be produced respectively, positive and negative polarization charge concentration area, also known as the piezoelectric potential, is the superposition of all dipole moments formed by the distribution of charge. The stress-induced charge polarity of piezoelectric polarization will result in energy band changes and thus potential barrier height, depletion layer modulation, and improved device performance [112, 115–117].

Duan et al. [118] successfully prepared flexible UV PDs based on ZnO semiconductor materials on PET substrates shown in Fig. 19a, b. In this experiment, when a stress of 0.2 was applied, the responsivity of the PD was increased by 20% and the sensitivity by 770%. The reason for this is that the charge on the ZnO/Au Schottky junction interface is redistributed by the piezoelectronic effect generated by the piezophoton effect of the piezoelectric element, which leads to a change in the Schottky barrier height and the depletion

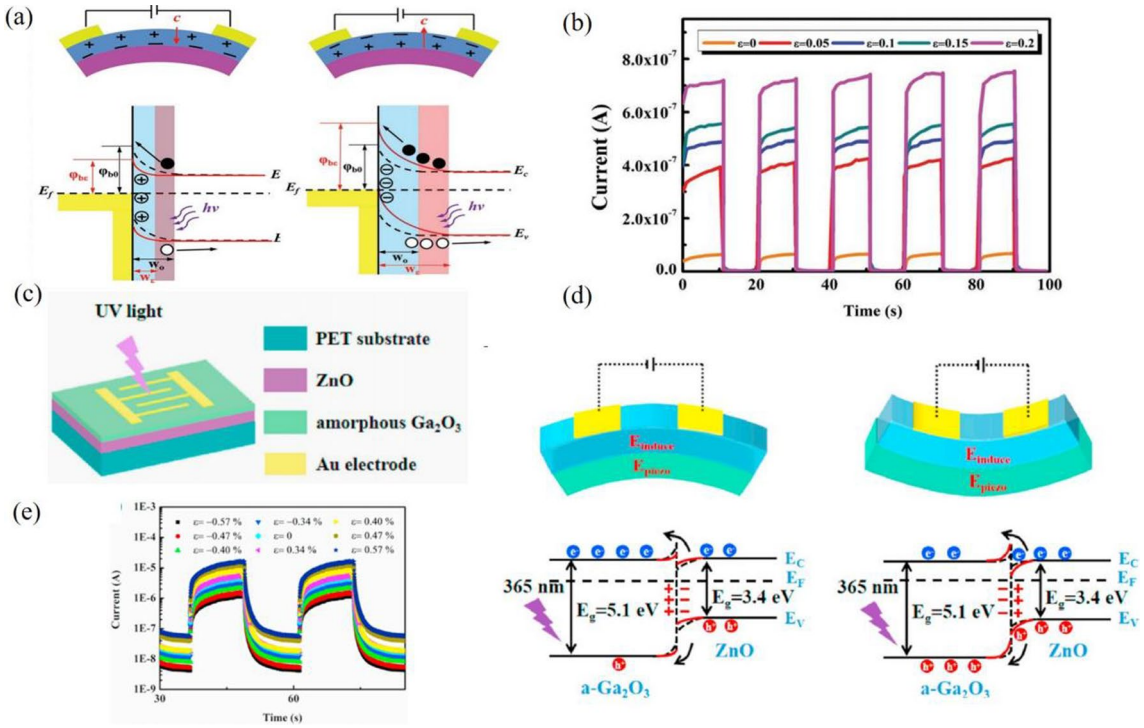

Fig. 19 **a** Schematic diagram and mechanism of Au/ZnO, **b** stability test under different bending strains [118], **c** schematic diagram of Au/a-Ga_2O_3/ZnO piezoelectric device [120], **d** energy band bending at a-Ga_2O_3/ZnO interface with strain, **e** device stability testing from different strain

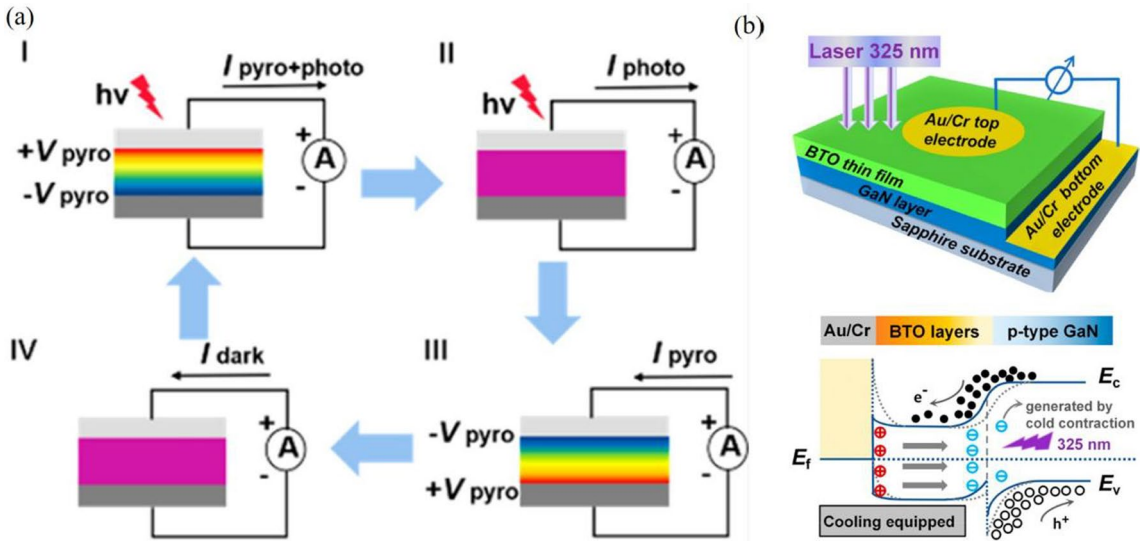

Fig. 20 a Schematic diagram of the four-step pyroelectric working mechanism [121], **b** schematic illustration of the self-powered BTO/GaN PD and the working mechanism in pyro-phototronic processes [124]

layer width, which has an effect on the transport of photogenerated carriers. The separation and transport of photogenerated electron–hole pairs are enhanced by the change of energy band structure and piezoelectric polarization at the ZnO/Au interface, and the device performance is improved. This provides an extended field for flexible UV pd's based on piezoelectric photovoltaics, which is important for optimizing and tuning the performance of UV PDs. Sun et al. [119] prepared dual-band AZO/MZO UV PD. The structure is a double-junction structure including two heterojunctions, MZO/Au and AZO/MZO, which enables dual-band detection. The responsivity and photocurrent are significantly improved by the piezoelectric effect.

The responsivity and photocurrent are significantly improved by the piezoelectric effect. Wang et al. [120] prepared a flexible MSM type UV detector by depositing ZnO and a-Ga_2O_3 layer on a PET substrate. The response of 2.49 A/W and detective of 1.98×10^{14} Jones are obtained when the tensile strain is 0.57%, which is improved by 283% and 620%, respectively. In addition, an optical response time is improved, and the detector maintains excellent stability and reliability. The mechanism of its related piezoelectric effect is shown in Fig. 19c, d.

5.2 Pyro-phototronic effect

Under periodic light irradiation, nanomaterials will deforms due to thermal expansion, generating a pyroelectric potential distributed along the c-axis of the crystal and pyroelectric polarization charges at the upper and lower interfaces of the material. On the heterojunction surface, the generation, transport, complexation and separation of photogenerated carriers can be regulated by the polarization charge, thus improving the photogenerated carrier transport [121–123]. It is realized by naturally coupling the light-induced pyroelectric effect, photonic excitations and semiconductor properties. This can also be used as an efficient method for carrier generation, separation and transportation. The working mechanism is shown in Fig. 20a [121]. An increase in nanomaterial temperature induces a sharp peak (I_{py+ph}), a stable current value (I_{ph}), a falling peak at the moment of switching off the light caused by the reverse pyroelectric potential, and a settled value (I_{dark}) [121]. As is shown in Fig. 20b, Zhang et al. [124] combined $BaTiO_3$ film with a GaN layer to form a heterojunction structure with thermal photoelectronic effect, realizing a high-efficiency self-powered $BaTiO_3$/GaN UV PD with high responsivity and fast response time. Combining the preparation of UV PDs with pyroelectric effects can achieve fast detection of UV radiation at room temperature, which opens up new optimization solutions for the preparation of PDs based on non-centrosymmetric materials. Nguyen et al. [125] prepared UV PDs based on p-n heterojunctions of Ag nanowires coated with ZnO/Cu_2O and ZnO /NiO, respectively. The heat loss of the device is reduced due to low thermal conductivity of CuO, and the light sensitivity is increased by reducing the thermal conductivity of the p-type layer. The optimized device has a responsivity of 0.98 A•W^{-1} and a detection rate of 1.62×10^{13} Jones. It will provide an important reference for future transparent ultraviolet light detection systems.

5.3 Ferroelectric effect

Ferroelectric effect is also characteristic of non-central symmetric crystals. It occurs when a material is stimulated by an external force, which can be changed by changing the applied electric field caused by the polarization direction reversal. Semiconductor materials with the ferroelectric effect are called ferroelectric materials, which includes $BaTiO_3$ [17], PVDF-TrFE [126] and PLZT [127] etc. Related studies have reported that metal oxide doped with V or Cr can also be converted into ferroelectric materials. As is shown in Fig. 21, Wang et al. [128] transformed ZnO into a ferroelectric material by doping with V to form a heterojunction with Ga_2O_3, and deposited Al electrodes to form a self-powered solar-blind UV PD with ferroelectric behavior. The ZnO:V induced ferroelectric polarization field can be used to regulate the width of depletion region through

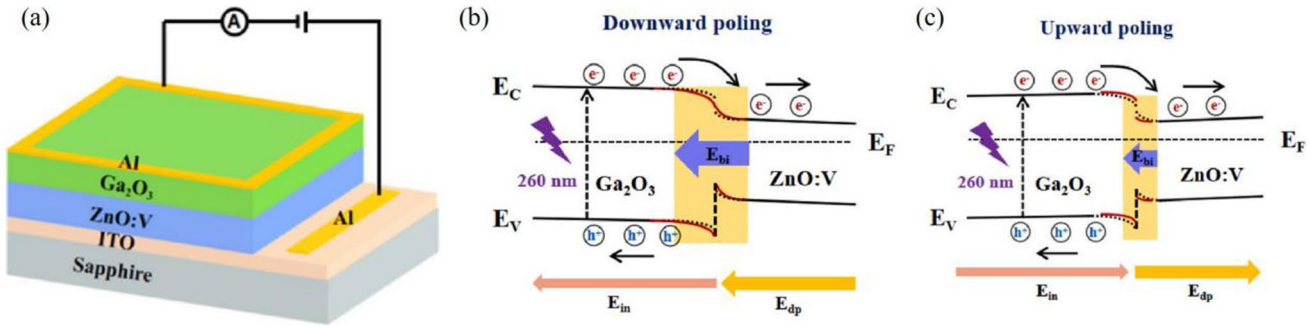

Fig. 21 **a** Structure diagram of the Al/Ga_2O_3/ZnO:V/ITO device, **b** the energy band diagram of Ga_2O_3/ZnO:V device, **c** upward poling state under 260 nm light at zero bias [128]

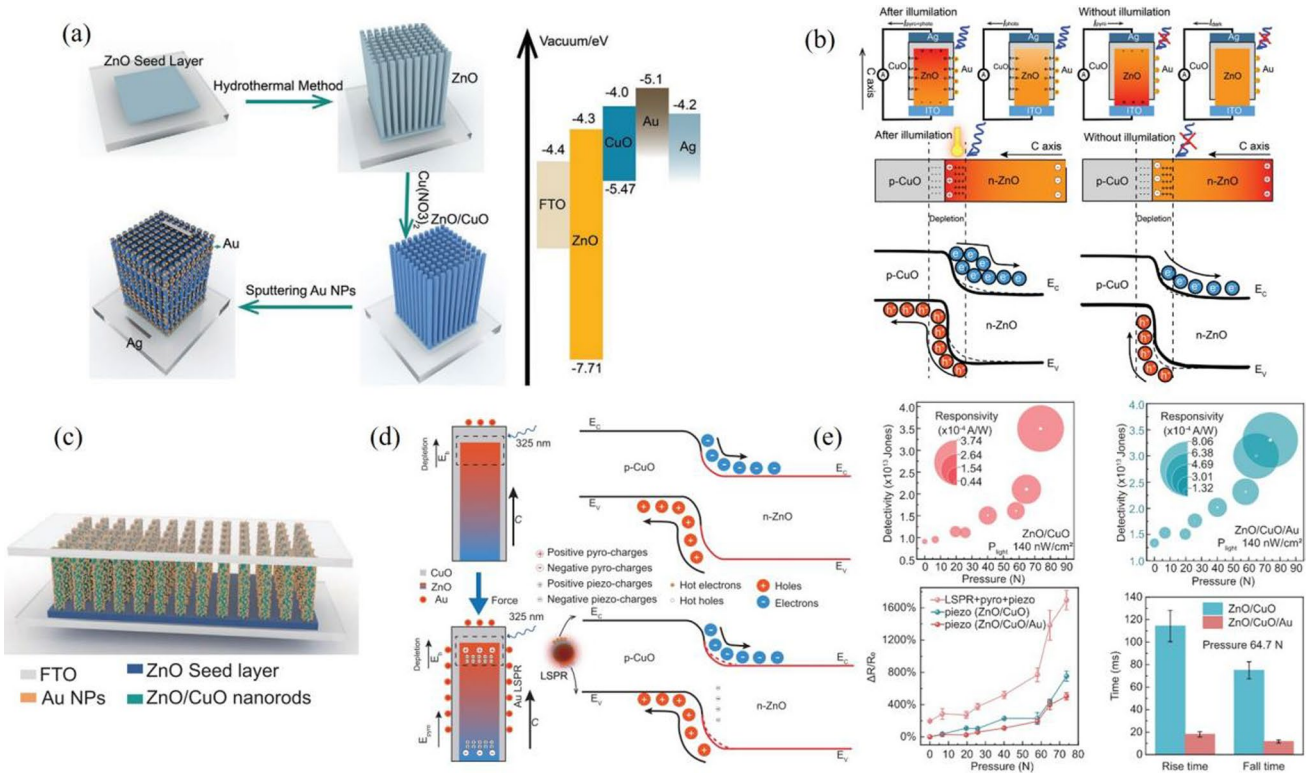

Fig. 22 **a** Structure and energy band diagram of the p-CuO/n-ZnO heterojunction device, **b** schematic illustration of the working mechanism of localized surface plasmon resonance effect-combined pyroelectric and photoexcitation processes, corresponding to the four stages of photoresponse [131], **c** schematic diagram of the device after coupling the piezoelectric effect and **d** comparison of its performance

the applied electric field to modulate the photogenerated carriers. The ferroelectric UV PDs are classified into three types, including ferroelectric depolarization field driven type, built-in electric field co-driven type, and ferroelectric field enhanced type [129]. The ability of a single ferroelectric material to separate photogenerated carriers is weak, so ferroelectric materials and other metal oxides are often formed into a heterojunction to enhance the separation of photogenerated carriers and improve the performance of the device through the synergistic effect of depolarization field and built-in electric field. It establishes a new direction for the investigation on UV PDs.

5.4 Coupling effect

The special properties of non-central symmetric crystals have been widely used to improve the performance of PDs. In recent years, the research on coupled-effect enhanced devices has been gradually deepened, and the use of coupled localized surface plasmon resonance effect and pyroelectric effect induced by metal nanoparticles to enhance the device performance has attracted wide attention. Huang et al. [130] combines the pyro-phototronic effect of ZnO with localized surface plasmon resonance effect of Ag nanoparticles to improve the performance of ZnO-based photodetectors. As is shown in Fig. 22a, Li et al. [131] sputtered Au nanoparticles layer on the ZnO/CuO heterojunction, and combined with the localized surface plasmon resonance and pyroelectric effect caused by Au nanoparticles to enhance the device performance. The mechanism of action is shown in Fig. 22b below, since the magnitude of pyroelectric current and the rate of change of temperature (dT/dt) are linearly related, the transient thermal power caused by the localized surface plasmon resonance effect can cause the temperature to rise, and the generated pyroelectric potential can be coupled with the built-in electric field to modulate the generation, recombination, separation and transport of photogenerated carriers. The sensitivity, responsiveness of the device have been improved. On this basis, Li et al. [132] coupled the piezoelectric effect based on previous work. As is plotted in Fig. 22c, d, under pressure, the rise and fall times of ZnO/CuO devices are reduced, and the responsiveness is improved. These results show that the coupling effect of localized surface plasmon resonance effect, thermal

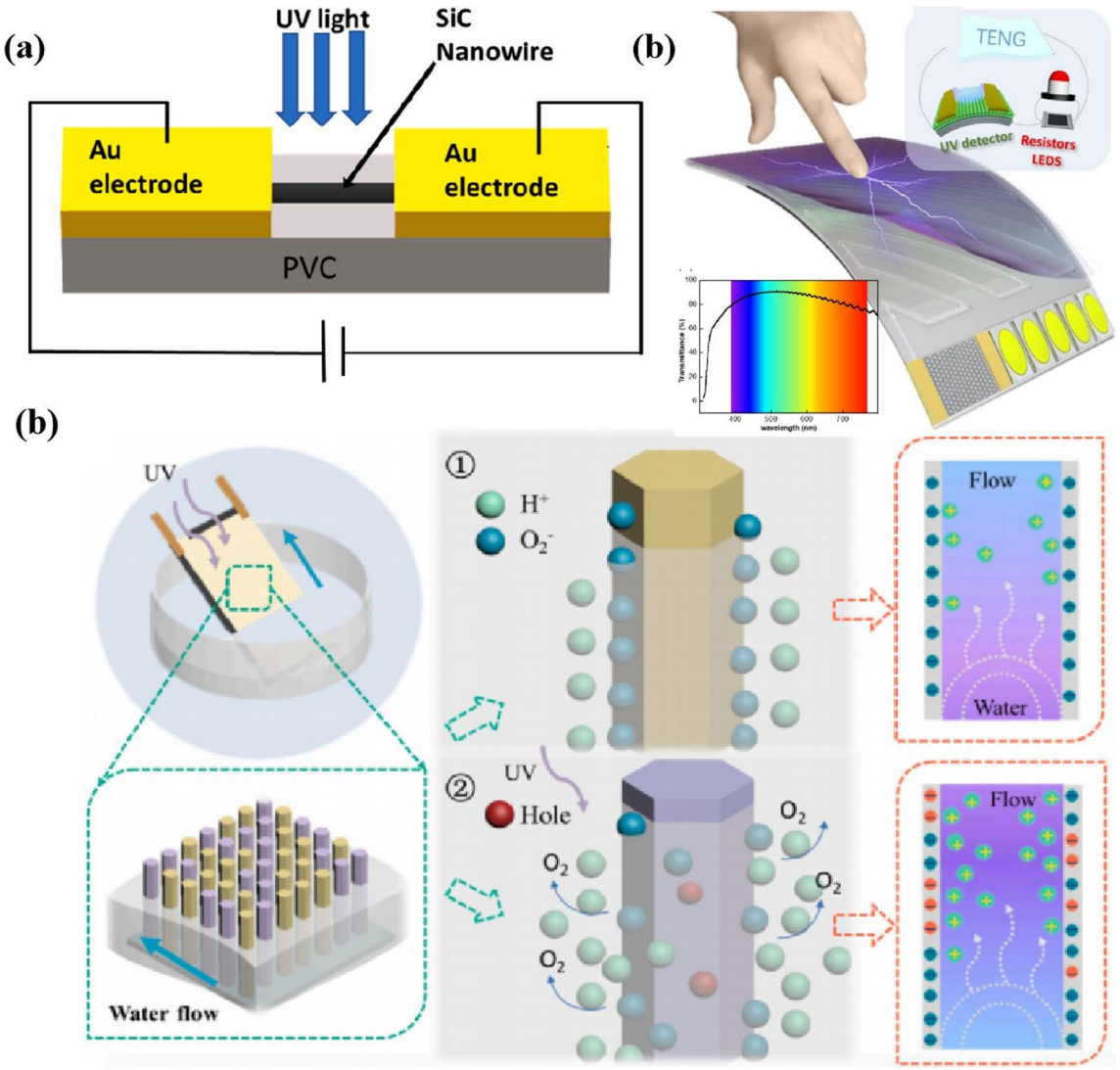

Fig. 23 **a** Schematic diagram of the flexible SiC UV PDs [134], **b** triboelectric nanogenerator-based triboelectric UV PD [136], **c** the mechanism of water flow in the natural environment as the basis of energy supply [138]

photoelectrons and piezoelectric photoelectrons improves the performance of PDs.

6 Application

6.1 Novel self-powered type PDs

Traditional UV radiation also requires an external power source to provide operating energy. However, its service life is limited, and needs to be checked and maintained regularly, consumable and does not meet the requirements of wearable devices [133]. Novel self-powered UV detector can realize the miniaturization, energy saving and meet the requirements of green and sustainable development, it will be the development trend of the next generation of UV PDs.

6.1.1 Photovoltaic effect

The main technology currently used to realize self-powered UV PDs is the photovoltaic effect. It mainly include Schottky-type [134], p–n junction structure and PECC-type, which can realize self-power due to the built-in electric field that will be formed on the contact surface of the semiconductor/metal or semiconductor/ semiconductor [135]. Under UV irradiation, the electrons and holes will move to the opposite direction under the built-in electric field, and this separation and transmission process will generate photocurrent. A flexible, self-powered and cost-effective single-nanowire UV PD based on SiC has been reported [134],

as is shown in Fig. 23a. The self-powered mechanism can be explained according to the Schottky contact. When SiC nanowires and Au electrodes are in contact, a built-in electric fields is generated to achieve self-power. UV detectors based on the photovoltaic effect usually show high responsivity, sensitivity and stability to UV radiation.

6.1.2 New self-powered strategy

With the deepening of research, novel self-powered methods have been realized, which enables powering of devices in a green, low-power form. There are various forms of energy in nature, and putting these energies to use in appropriate forms is a focus of current research. Zhang et al. [136] focused on an emerging strategy of harvesting human motion energy to trigger the PDs, as is shown in Fig. 23a, b. Self-powered real-time UV PDs is realized by coupling triboelectric effect and electrostatic induction technology and impedance matching effect between friction nano-generator and sensor.

Recently, it has been discovered that nano-generators can harvest energy from natural environments, such as water, which has become a new research point [137]. Guan et al. [138] reported a novel UV PD without external power supply based on photovoltaic coupling and ZnO nanowire array photoelectric effect, which uses natural water as the basis of energy supply, as is plotted in Fig. 23c. When ultraviolet is irradiated, water flows on the nanowire array and evaporation, energy is generated, and the output current can be used as detection signal.

6.2 Wearable UV PDs

Wearable devices mainly refer to portable devices that are capable of analyzing information about the environment or human signs [139]. In recent years, due to the hole in the ozone layer, the intensity of UV light has increased, so the preparation of devices that can detect the intensity of UV light has become a current concern. Flexible UV PDs have also been applied to wearable devices, making it possible to detect the intensity of UV light in real time during outdoor sports. Flexible wearables have already applied in various fields of daily life, such as sports bracelets and health testing etc. Some UV-sensitive semiconductor layers are integrated on flexible substrates to realize flexible UV detector devices. Xu et al. [140] constructed p-CuZnS/n-TiO_2 heterojunction and prepared a flexible self-powered UV PD. Instead of using conventional titanium foil as a substrate, the device is effectively replaced by a network of titanium fibers compiled from thin titanium wires, allowing the device to change its rigid planar morphology for integration with commercial electronic devices, and bending and stretching does not affect the device performance, allowing for better application in wearable devices. It has a strong response to UV radiation (640 $A \bullet W^{-1}$) and is capable of generating a large photocurrent. The prepared UV PDs are integrated into a designed circuit to constitute UV photoelectric

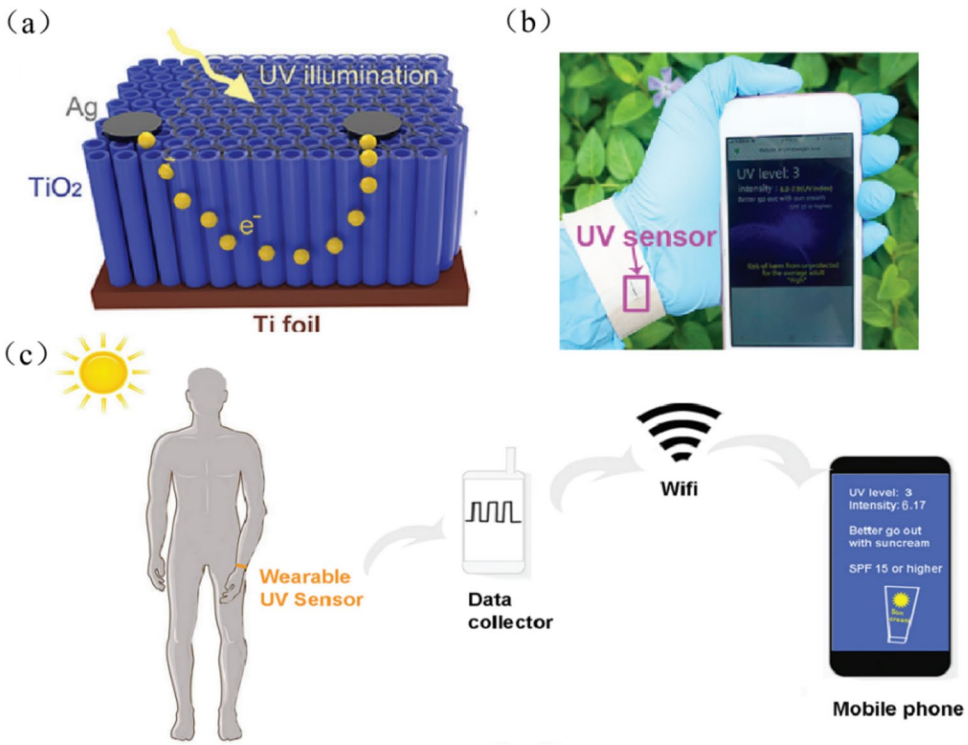

Fig. 24 **a** Schematic illustration of p-CuZnS/n-TiO_2 NTAs with Ag contacts device, **b** wearable real-time UV sensor, (c) Practical application [140]

radiation monitoring meter, and a real-time UV photoelectric monitoring wearable device is formed by combining with a sports bracelet or clothes, which can monitor the UV light in real time and transmit the data to a smartphone via a wireless network. This provides a reference for the development of wearable UV detectors (Fig. 24). Tran et al. [141] constructed a UV PDs based on a stable wide bandgap zirconium-benzene dicarboxylate metal–organic thin film. Due to the difficulty and time-consuming preparation of the conventional zirconium-benzene dicarboxylate film, they use a continuous layer-by-layer spin-coating method to prepare a high-quality zirconium-benzene dicarboxylate thin film as the light-absorbing layer. The device has a specific detection rate of 7.85×10^{10} Jones at zero bias and a rise/fall time of 80/150 ms. In addition, the device can quickly identify the high risk of UV exposure by measuring UV intensity, without relying on weather forecasts. In addition, researchers use the UV intensity information collected by those who work outdoors to explore the effect of UV light on the human body.

7 Conclusions and outlook

With the development of the aerospace and semiconductor industries, the demand for UV PDs is showing a sustained growth trend, and the fabrication of high-performance UV PDs is necessary. This review provides a detailed summary of the development of UV PDs in recent years, which includes the basic concepts, main performance parameters, various design structures, related materials, and various performance effects. For non-centrosymmetric semiconductor materials, piezoelectric, ferroelectric and pyroelectric effects can be used to modulate the device performance by adjusting the transport of photogenerated carriers, which has been the focus of recent research. Combining the plasmonic excitation with the pyroelectric and piezoelectric effects, the detection ability of the device for weak UV light has been enhanced by 2–3 orders of magnitude. Promoting the green and sustainable development of science and technology is the current issue, it is necessary to investigate on easily accessible and non-polluting optoelectronic materials. Biomass materials have attracted the attention of researchers, and related studies have shown that DNA biomolecules can achieve high conversion efficiency of UV to hole transport [[142]]. Combining DNA biomolecules with optoelectronic semiconductor materials to form eco-friendly and organic bio-hybrid optoelectronic devices has become a new research direction. Wearable flexible UV detector is also a research hotspot, but most of the existing flexible sensors are constructed on a closed polymer film substrate, which is not flexible enough and is not breathable. This will greatly reduce wearing comfort, and the sweat secreted by the skin during long-term wear can cause destructive erosion of sensor components. Therefore, it is crucial to choose hydrophobic and breathable flexible material. In addition, future research on wearable sensors will focus on integrating multiple functional devices to achieve multifunctional detection. In recent years, dual function sensors have been developed by integrating UV and temperature sensing on the same flexible substrate. However, most of the existing bifunctional sensors utilize the same sensitive material, which will output variable electrical signals when they are excited by external UV light or temperature. This poses a serious challenge for tracking and decoupling electrical signals source. In summary, the research on UV PDs has achieved fruitful results, but still faces various difficulties and challenges. This review provides a comprehensive introduction about UV PDs, providing a reference for future research and development of UV PDs.

Acknowledgements This work was supported by the National Natural Science Foundations of China (Grant No. 11804273), Natural Science Foundation of Shaanxi Province, China (Grant No. 2024JC-YBMS-060), Key Research and Development Projects of Shaanxi Province (Grant No. 2019GY-170), Postgraduate Innovative and Practical Ability Training Program of Xi'an Shiyou University (Grant No. YCS23113100).

Authors contributions All authors contributed to the study conception and design. Data collection and analysis were performed by Jijun Ding, Pengfei Zhao, and Haixia Chen. The first draft of the manuscript was written by Jijun Ding and Pengfei Zhao, and all authors commented on previous versions of the manuscript. All authors read and approved the final manuscript.

Funding National Natural Science Foundation of China, 11804273, Haixia Chen, Key Research and Development Projects of Shaanxi Province, 2019GY-170, Jijun Ding, Natural Science Foundation of Shaanxi Province, 2024JC-YBMS-060, Jijun Ding.

Data availability Data sharing not applicable to this article as no datasets were generated or analyzed during the current study.

Declarations

Conflict of interest The authors have no competing interests to declare that are relevant to the content of this article.

References

1. N. Kuma, M. Patel, J. Kim, C. Jeong, C.P. Wong, Flexible transparent photovoltaics for ultra-UV photodetection and functional UV-shielding based on Ga_2O_3/Cu_2O heterojunction. Appl. Mater. Today **29**, 101620 (2022). https://doi.org/10.1016/j.apmt.2022.101620
2. J.G. Liu, W. He, L. Zhou, F. Yang, Application of ultraviolet detector in discharge detection. Int J. Emerg. Electr. **7**, 1 (2006). https://doi.org/10.2202/1553-779X.1322

3. W. Zheng, R.C. Lin, J.X. Ran, Z.J. Zhang, X. Ji, F. Huang, Vacuum-ultraviolet photovoltaic detector. ACS Nano **12**, 425 (2018). https://doi.org/10.1021/acsnano.7b06633
4. T. Zhan, J.W. Sun, T. Feng, Y.L. Zhang, B.R. Zhou, B.H. Zhang, J.X. Wang, P. Sarro, G.Q. Zhang, Z.W. Liu, X.Y. Yi, J.M. Li, Electrical characteristics and photodetection mechanism of TiO_2/AlGaN/GaN heterostructure-based ultraviolet detectors with a Schottky junction. J. Mater. Chem. C **11**, 1704 (2023). https://doi.org/10.1039/D2TC04491A
5. C.G. Núñez, A. Vilouras, W.T. Navaraj, F.Y. Liu, R. Dahiya, ZnO nanowires-based flexible UV PD system for wearable dosimetry. IEEE Sens. J. **18**, 7881 (2018). https://doi.org/10.1109/JSEN.2018.2853762
6. J. Park, J. Lee, Y. Noh, K.H. Shin, D.J. Lee, Flexible ultraviolet PDs with ZnO nanowire networks fabricated by large area controlled roll-to-roll processing. J. Mater. Chem. C **4**, 7948 (2016). https://doi.org/10.1039/C6TC02371A
7. P. Gu, X.H. Zhu, D.Y. Yang, Effect of annealing temperature on the performance of photoconductive ultraviolet detectors based on ZnO thin films. Appl. Phys. A **125**, 1 (2019). https://doi.org/10.1007/s00339-018-2361-3
8. D.T. You, C.X. Xu, J. Zhao, F.F. Qin, W. Zhang, R. Wang, Z.L. Shi, Q.N. Cui, Single-crystal ZnO/AlN core/shell nanowires for ultraviolet emission and dual-color ultraviolet detection. Adv. Opt. Mater. **7**, 1801522 (2019). https://doi.org/10.1002/adom.201801522
9. C. Saricam, N. Okur, İ Göcek, Functionalization of electrospun nanofibers by using titanium dioxide and 1,3,7-Trimethyl xanthine for developing ultraviolet protection. J. Ind. Text. **50**, 398 (2019). https://doi.org/10.1177/1528083719831088
10. L. Horton, A.E. Torres, S. Narla, A.B. Lyons, I. Kohli, J.M. Gelfand, D.M. Ozog, I.H. Hamzavi, H.W. Lim, Spectrum of virucidal activity from ultraviolet to infrared radiation. Photochem. Photobiol. Sci. **19**, 1262 (2020). https://doi.org/10.1039/d0pp00221f
11. Z. Zhang, Y. Geng, S.Q. Cao, C. Zheng, H.F. Gao, X.B. Zhu, X.S. Zhang, Y.C. Wu, Ultraviolet PDs based on polymer microwire arrays toward wearable medical devices. ACS Appl. Mater. Interfaces **14**, 41257 (2022). https://doi.org/10.1021/acsami.2c04169
12. B.I. Veleva, R.L.V. Bezooijen, V.G.M. Chel, M.E. Numans, M.A. Caljouw, Effect of ultraviolet light on mood, depressive disorders and well-being. Photodermatol. Photoimmunol. Photomed. **34**, 288 (2018). https://doi.org/10.1111/phpp.12396
13. Y.Z. Liu, T. Zhang, L.Y. Shen, H.S. Wu, N. Wang, F.Z. Wang, X.H. Pan, Z.Z. Ye, Self-powered flexible ultraviolet PDs based on CuI/a-ZTO heterojunction processed at room temperature. ACS Appl. Mater. Interfaces **15**, 29267 (2023). https://doi.org/10.1021/acsami.3c03600
14. J. Han, J.H. Lee, S.H. Ju, Fabrication of flexible ultraviolet PDs using an all-spray-coating process. AIP Adv. **6**, 045218 (2016). https://doi.org/10.1063/1.4948460
15. J.K. Li, C. Ge, K.J. Jin, J.Y. Du, J.T. Yang, H.B. Lu, G.G. Yang, Self-driven visible-blind PD based on ferroelectric perovskite oxides. Appl. Phys. Lett. **110**, 142901 (2017). https://doi.org/10.1063/1.4979587
16. T. Li, W.Q. Song, R.Q. Wan, L. Zhang, J.C. Yan, W.H. Zhu, 3D-MSM AlN deep ultraviolet detector. IEEE J. Quantum Electron. **57**, 1 (2021). https://doi.org/10.1109/JQE.2021.3075543
17. Z. Lou, G.Z. Shen, Flexible PDs based on 1D inorganic nanostructures. Adv. Sci. **3**, 1500287 (2016). https://doi.org/10.1002/advs.201500287
18. J.F. Chao, X.Y. Sun, S.M. Xing, X.T. Zhang, S.L. Gao, Z.Y. Du, Thermal calcination fabrication of porous tin dioxide for new flexible ultraviolet PDs. J. Alloy. Compd. **753**, 212 (2018). https://doi.org/10.1016/j.jallcom.2018.04.228
19. Y. Li, Y.H. Li, J. Chen, Z.P. Sun, Z. Li, X. Han, P. Li, X.J. Lin, R.Q. Liu, Y.W. Ma, W. Huang, Full-solution processed all-nanowire flexible and transparent ultraviolet PDs. J. Mater. Chem. C **6**, 11666 (2018). https://doi.org/10.1039/C8TC04044C
20. J.D. Hao, L. Li, P. Gao, X.Q. Jiang, C.C. Ban, N.Q. Shi, Deep ultraviolet detectors based on wide bandgap semiconductors: a review. J. Nanopart. Res. **25**, 81 (2023). https://doi.org/10.1007/s11051-023-05694-6
21. P. Rong, S. Ren, Q. Yu, Fabrications and applications of ZnO nanomaterials in flexible functional devices: a review. Anal. Chem. **49**, 336 (2019). https://doi.org/10.1080/10408347.2018.1531691
22. M. Zhang, D.M. Li, J.R. Zhou, W.Y. Chen, S.P. Ruan, Ultraviolet detector based on TiO_2 nanowire array-polymer hybrids with low dark current. J. Alloy. Compd. **618**, 23 (2015). https://doi.org/10.1016/j.jallcom.2014.07.040
23. X.M. Bian, J.W. Zhang, Fast-response photoconductive metal-semiconductor-metal ultraviolet detector based on ZnO film grown by radio-frequency magnetron sputtering. Opt. Eng. **47**, 064001 (2008). https://doi.org/10.1117/1.2939091
24. C.Y. Liu, B.P. Zhang, Z.W. Lu, N.T. Binh, K. Wakatsuki, Y. Segawa, R. Mu, Fabrication and characterization of ZnO film based UV PD. J. Mater. Sci. **20**, 197 (2008). https://doi.org/10.1007/s10854-008-9698-x
25. M. Xi, X.X. Wang, Y. Zhao, X. Min, X.X. Wang, Y. Zhao, Z.T. Zhu, H. Fong, Electrospun ZnO/SiO_2 hybrid nanofibrous mat for flexible ultraviolet sensor. Appl. Phys. Lett. **104**, 133102 (2014). https://doi.org/10.1063/1.4870296
26. C.T. Wu, A.A. Soliman, H. Sugimura, T. Utsunomiya, T. Ichii et al., Formation of submicron-sized silica patterns on flexible polymer substrates based on vacuum ultraviolet photo-oxidation. RSC Adv. **9**, 32313 (2019). https://doi.org/10.1039/C9RA07256J
27. P. Xiao, H.J. Gwak, S. Seo, Fabrication of a flexible PD based on a liquid eutectic Gallium Indium. Mater. **13**, 5210 (2020). https://doi.org/10.3390/ma13225210
28. Y.N. Zou, Y. Zhang, Y.M. Hu, H.S. Gu, Ultraviolet detectors based on wide bandgap semiconductor nanowire: A Review. Sensors **18**, 2072 (2018). https://doi.org/10.3390/s18072072
29. W.X. Ouyang, J.X. Chen, Z.F. Shi, X.S. Fang, Self-powered UV photodetectors based on ZnO nanomaterials. Appl. Phys. Rev. **8**, 031315 (2021). https://doi.org/10.1063/5.0058482
30. X.L. Su, Y. Li, M.Y. Zhang, P. Hu, M.F. Guo, A.X. Li, Y. Zhang, Q. Li, F. Yun, GaN ultraviolet photodetector with petal-like β-Ga_2O_3 microcrystalline layer. AIP Adv. **10**, 125107 (2020). https://doi.org/10.1063/5.0028550
31. S.Y. Feng, Z.T. Liu, L.Z. Feng, J.C. Wang, H.N. Xu, L.J. Deng, O.X. Zhou, X. Jiang, B.D. Liu, X.L. Zhang, High-performance self-powered ultraviolet photodetector based on Ga_2O_3/GaN heterostructure for optical imaging. J. Alloy. Compd. **945**, 169274 (2023). https://doi.org/10.1016/j.jallcom.2023.169274
32. H.W. Xie, C.X. Kang, M.A. Iqbal, X.L. Weng, K.W. Wu, W. Tang, L. Qi, Y.J. Zeng, Ferroelectric tuning of ZnO ultraviolet photodetectors. Nanomaterials **12**, 3358 (2022). https://doi.org/10.3390/nano12193358
33. X.H. Zhao, Y. Tao, J.X. Dong, Y.C. Fang, X.X. Song, Z.X. Yan, $Cs_3Cu_2I_5$/ZnO heterostructure for flexible visible-blind ultraviolet photodetection. ACS Appl. Mater. Interfaces **14**, 43490 (2022). https://doi.org/10.1021/acsami.2c11202
34. X.M. Zhang, F.B. Ji, G. Wang, J. Li, M.J. Jin, J.Y. Zhou, E.Q. Xie, X.J. Pan, 360° detection of linear ZnO@CFs photoelectrochemical-type ultraviolet PD. Appl. Phys. Lett. **123**, 031105 (2023). https://doi.org/10.1063/5.0158841
35. L. Duan, F.N. He, Y. Tian, F.N. He, Y. Tian, B. Sun, J.B. Fan, X.C. Yu, L. Ni, Y. Zhang, Y.N. Chen, W.X. Zhang, Fabrication

of self-powered fast-response ultraviolet PDs based on Graphene/ZnO: Al nanorod-array-film structure with stable schottky barrier. ACS Appl. Mater. Interfaces **9**, 8161 (2017). https://doi.org/10.1021/acsami.6b14305
36. L.L. Chu, C. Xu, W. Zeng, C. Nie, L.T. Deng, F. Lei, Performance enhanced of metal-semiconductor-metal ultraviolet PD enabled by ZnO/MXene/ZnOsandwich structure achieved through the hot-electrons injection in MXene nanoflakes. IEEE Trans. Electron Devices **69**, 6811 (2022). https://doi.org/10.1109/TED.2022.3212328
37. J. Huang, B. Li, Y. Hu, X.Y. Zhou, Z.L. Zhang, Y.C. Ma, K. Tang, L.J. Wang, Y.C. Lu, Transparent p-NiO/n-ZnO heterojunction ultraviolet PDs prepared on flexible substrates. Surf. Coat. Technol. **362**, 57 (2019). https://doi.org/10.1016/j.surfcoat.2019.01.099
38. D.K. Kwon, S.J. Lee, J.M. Myoung, High-performance flexible ZnO nanorod UV PDs with a network-structured Cu nanowire electrode. Nanoscale **8**, 16677 (2016). https://doi.org/10.1039/C6NR05256H
39. L. Zhang, N.M. Li, Q.C. Ma, J.H. Ding, C. Chen, Z.C. Hu, W.W. Zhao, Y.F.G. Li, H.H. Feng, M.Y. Li, H.J. Ji, Large-area flexible and transparent UV PD based on cross-linked Ag NW@ZnO NRs with high performance. J. Mater. Sci. Technol. **110**, 65 (2022). https://doi.org/10.1016/j.jmst.2021.08.037
40. S.Y. Wang, R.S. Chen, Y. Ren, Y.W. Hu, Z.Q. Yang, C.J. Zhou, Y.J. Lv, X. Lu, Highly-rectifying Graphene/GaN Schottky contact for self-powered UV PD. IEEE Photonics Technol. Lett. **33**, 213 (2021). https://doi.org/10.1109/LPT.2021.3052171
41. H. Li, L.M. Zhao, J.P. Meng, C.F. Pan, Y. Zhang, Y.M. Zhang, Z. Liu, Y. Zou, Y.B. Fan, Z.L. Wang, Z. Li, Triboelectric-polarization-enhanced high sensitive ZnO UV sensor. Nano Today **33**, 100873 (2020). https://doi.org/10.1016/j.nantod.2020.100873
42. T.T. Gao, Y. Ji, Y. Yang, Thermo-phototronic effect enhanced PDs based on porous ZnO materials. Adv. Electron. Mater. **5**, 1900776 (2019). https://doi.org/10.1002/aelm.201900776
43. Y.F. Li, S.D. Wang, Y.Z. Guan, J. Feng, H.F. Zhang, S.P. Ruan, L.H. Chen, K.X. Liu, C.X. Liu, J.R. Zhou, MSM ultraviolet detectors based on Zr01Ti09O2 solid solution. Integr. Ferroelectr. **138**, 94 (2012). https://doi.org/10.1080/10584587.2012.688471
44. B.G. Hunashimarad, J.S. Bhat, P.V. Raghavendra, R.F. Bhajantri, ZnO: Ca MSM ultraviolet photodetectors. Opt. Mater. **124**, 111960 (2022). https://doi.org/10.1016/j.optmat.2021.111960
45. N. Fathima, N. Pradeep, J. Balakrishnan, Investigations of the effects of electrode geometry and mechanical stress on antimony doped zinc oxide nanostructures based MSM UV PDs fabricated on flexible substrates. Sol. Energy Mater. Sol. Cells **194**, 207 (2019). https://doi.org/10.1016/j.solmat.2019.02.016
46. Y.H. Luo, Y. Zhang, X. Li, H.H. Jiang, M.Z. Xiao, C. Wen, Y.K. Xing, X.J. Li, Self-powered ultraviolet PD with very short and balanced response/recovery time based on ZnO/Si heterojunction with complex interface structure. Mater. Chem. Phys. **302**, 127520 (2023). https://doi.org/10.1016/j.matchemphys.2023.127520
47. Z. Lou, X.L. Yang, H.R. Chen, Z.Z. Liang, Flexible ultraviolet PDs based on ZnO-SnO_2 heterojunction nanowire arrays. J. Semicond. **39**, 024002 (2018). https://doi.org/10.1088/1674-4926/39/2/024002
48. Y. Li, X.J. Wei, Q.Y. Yang, J. Zhang, W.C. Wang, L.L. Dong, B.K. Gao, C. Li, X.L. Sun, Y.W. Ma, Fast-response self-powered flexible transparent ultraviolet PDs based on a CuO/ZnO nanowire array heterojunction. New J. Chem. **47**, 6397 (2023). https://doi.org/10.1039/D2NJ06004C
49. D. Wang, P. Shi, R.F. Xing, Z.F. Wu, L. Wei, Y.X. Chen, H.X. Ren, C.F. Yu, F.J. Li, Self-powered ZnO/$SrCoO_x$ flexible ultraviolet detectors processed at room temperature. Mater. Des. **203**, 109616 (2021). https://doi.org/10.1016/j.matdes.2021.109616
50. C.S. Chen, B.F. Hu, Z. Wang, X.Q. Lv, C.Q. Zhang, B.B. Chen, H.S. San, W. Hofmann, Face-to-face intercrossed ZnO nanorod arrays with extensive NR-NR homojunctions for a highly sensitive and self-powered ultraviolet photodetector. Nano Energy **65**, 106042 (2019). https://doi.org/10.1016/j.nanoen.2019.104042
51. Y.M. Wang, Y. Chen, W.Q. Zhao, L.W. Ding, L. Wen, H.X. Li, F. Jiang, J. Su, L.Y. Li, N.S. Liu, Y.H. Gao, A self-powered fast-response ultraviolet detector of p-n homojunction assembled from two ZnO-based nanowires. Nano-Micro Lett. **9**, 1 (2017). https://doi.org/10.1007/s40820-016-0112-6
52. K. Tang, M.M. Jiang, B.W. Yang, T. Xu, Z. Liu, P. Wan, C.X. Kan, D.N. Shi, Enhancing UV photodetection performance of an individual ZnO microwire p-n homojunction via interfacial engineering. Nanoscale **15**, 2292 (2023). https://doi.org/10.1039/D2NR06431F
53. J. Li, R. Wang, Z.W. Bai, G. Wang, X.M. Zhang, J.S. Yuan, J.Y. Zhou, E.Q. Xie, X.J. Pan, Enhanced performance of photoelectrochemical type ultraviolet PD by constructing a $KNbO_3$/ZnO heterojunction. Sens. Actuators, A **358**, 114434 (2023). https://doi.org/10.1016/j.sna.2023.114434
54. C. Xu, J.J. Ding, H.X. Chen, X.J. Wang, Plasma etched Ag nanospheres for large increases of ZnO fluorescence emission: a combined theoretical-experimental study. Ceram. Int. **49**, 13208 (2023). https://doi.org/10.1016/j.ceramint.2022.12.200
55. H. Jang, D.K. Kwon, D.H. Kim, J.M. Myoung, Characteristics of flexible ZnO nanorod UV PDs processed by using a direct silicon etching transfer method. J. Mater. Chem. C **10**, 6805 (2022). https://doi.org/10.1039/D2TC00377E
56. S.M. Saleh, A. Khazali, H.S. Al-Salman, A. Hmood, Low cost flexible ultraviolet PD based on ZnO nanorods prepared using chemical bath deposition. Mater. Lett. **277**, 128177 (2020). https://doi.org/10.1016/j.matlet.2020.128177
57. H.F. Dai, J.J. Ding, H.X. Chen, Haiwei Fu, Improvement of ethanolamine sensing performance based on Au-modified ZnO rod-like nanoflowers. Mater. Lett. **340**, 134183 (2023). https://doi.org/10.1016/j.matlet.2023.134183
58. Y.Y. Zeng, X.H. Pan, B. Lu, Z.Z. Ye, Fabrication of flexible self-powered UV detectors based on ZnO nanowires and the enhancement by the decoration of Ag nanoparticles. RSC Adv. **6**, 31316 (2016). https://doi.org/10.1039/C6RA02922A
59. Q. Xu, L. Cheng, L.X. Meng, Z. Wang, S. Bai, X.Q. Tian, X.F. Jia, Y. Qin, Flexible self-powered ZnO film UV sensor with a high response. ACS Appl. Mater. Interfaces **11**, 26127 (2019). https://doi.org/10.1021/acsami.9b09264
60. P.P. Chen, T. Hang, Simple template-mediated fabrication of ZnO nanotube arrays and their application in flexible ultraviolet PDs. ACS Appl. Nano Mater. **6**, 1948 (2023). https://doi.org/10.1021/acsanm.2c04895
61. S.J. Young, Y.H. Liu, M.D. Nahin Islam Shiblee, K. Ahmed, L.T. Lai, L. Nagahara, T. Thundat, T. Yoshida, S. Arya, H. Furukawa, A. Khosla, Flexible ultraviolet PDs based on one-dimensional gallium-doped zinc oxide nanostructures. ACS Appl. Electron. Mater. **2**, 3522 (2020). https://doi.org/10.1021/acsaelm.0c00556
62. D.W. Yang, H.L. Ma, J.Q. Li, H.J. Fang, H.D. Xie, Sunscreen-inspired ZnO/PEG composites for flexible ultraviolet PDs with a giant on–off ratio. ACS Photonics **10**, 1320 (2023). https://doi.org/10.1021/acsphotonics.2c01959
63. D. Kuang, Y. Li, Y.F. Gao, J. Guo, X. Li, S. Xu, B. Liu, X.W. Liu, Y. Zhang, Z.N. Yu, Performance improvement of flexible ultraviolet PDs based on ZnO nanorod arrays by hydrothermal method with assistance of polyethyleneimine. J. Alloy. Compd. **899**, 163185 (2022). https://doi.org/10.1016/j.jallcom.2021.163185

64. S. Mondal, S. Ghosh, D. Basak, Extraordinarily high ultraviolet photodetection by defect tuned phosphorus doped ZnO thin film on flexible substrate. Mater. Res. Bull. **144**, 111490 (2021). https://doi.org/10.1016/j.materresbull.2021.111490
65. J.K. Li, C. Ge, K.J. Jin, J.Y. Du, J.T. Yang, H.B. Lu, G.Z. Yang, Photovoltaic and flexible deep ultraviolet wavelength detector based on novel beta-Ga(2)O(3)/muscovite heteroepitaxy. Sci. Rep. **10**, 16098 (2020). https://doi.org/10.1038/s41598-020-73112-1
66. S.R. Zhou, X. Peng, H.W. Liu, Z.F. Zhang, L.J. Ye, H.L. Li, Y.Q. Xiong, L.B. Niu, F.L. Chen, L. Fang, C.Y. Kong, W.J. Li, X. Yang, H. Zhang, Flexible solar-blind Ga_2O_3 ultraviolet PDs with high responsivity and photo-to-dark current ratio. IEEE Photonics J. **11**, 1 (2019). https://doi.org/10.1364/OME.449496
67. S. Qi, J.H. Liu, J.Y. Yue, X.Q. Ji, J.Y. Shen, Y.T. Yang, J.J. Wang, S. Li, Z.P. Wu, W.H. Tang, An enhanced ultrasensitive solar-blind UV PD based on an asymmetric Schottky junction designed with graphene/β-Ga_2O_3/Ag. J. Mater. Chem. C **11**, 8454 (2023). https://doi.org/10.1039/D3TC01456H
68. H.W. Xue, Q.M. He, G.Z. Jian, S.B. Long, T. Pang, M. Liu, An overview of the ultrawide bandgap Ga_2O_3 semiconductor-based schottky barrier diode for power electronics application. Nanoscale Res. Lett. **13**, 1 (2018). https://doi.org/10.1186/s11671-018-2712-1
69. J. Zhang, F.J. Liu, D. Liu, Y.X. Yin, M.X. Wang, Z.X. Sa, L. Sun, X.X. Zheng, X.M. Zhuang, Z.T. Lv, W.X. Mu, Z.T. Jia, Y. Tan, F. Chen, Z.X. Yang, Toward smart flexible self-powered near-UV PD of amorphous Ga_2O_3 nanosheet. Mater. Today Phys. **31**, 100997 (2023). https://doi.org/10.1016/j.mtphys.2023.100997
70. J.Y. Wei, L.P. Shen, Z.C. Zheng, Y.C. Xu, H. Wu, H. Zhou, H. Wang, The suppression of dark current for achieving high-performance Ga_2O_3 nanorod array ultraviolet PD. Ceram. Int. **48**, 12112 (2022). https://doi.org/10.1016/j.ceramint.2022.01.071
71. T. He, Y.K. Zhao, X.D. Zhang, W.K. Lin, K. Fu, C. Sun, F.F. Shi, X.Y. Ding, G.H. Yu, K. Zhang, S.L. Lu, X.P. Zhang, B.S. Zhang, Solar-blind ultraviolet PD based on graphene/vertical Ga_2O_3 nanowire array heterojunction. Nanophotonics **7**, 1557 (2018). https://doi.org/10.1515/nanoph-2018-0061
72. W.H. Zhu, L.X. Xiong, J.W. Si, Z.L. Hu, X. Gao, L.Y. Long, T. Li, R.Q. Wan, L. Zhang, L.C. Wang, Influence of deposition temperature on amorphous Ga_2O_3 solar-blind ultraviolet PD. Semicond. Sci. Technol. **35**, 055037 (2020). https://doi.org/10.1088/1361-6641/ab6ac1
73. C. Zhang, K.W. Liu, Q. Ai, X. Sun, X. Chen, J.L. Yang, Y.X. Zhu, Z. Cheng, B.H. Li, L. Liu, D.Z. Shen, High-performance fully transparent Ga_2O_3 solar-blind UV PD with the embedded indium–tin–oxide electrodes. Mater. Today Phys. **33**, 101034 (2023). https://doi.org/10.1016/j.mtphys.2023.101034
74. G.W. Li, K. Zhang, Y.T. Wu, A.X. Zhu, X. Fu, L. Wang, S.L. Feng, W.Q. Lu, Self-powered solar-blind ultraviolet PDs with Ga_2O_3 nanowires as the interlayer. Vacuum **215**, 112277 (2023). https://doi.org/10.1016/j.vacuum.2023.112277
75. Y.F. Wang, Y.X. Xue, J. Su, Z.H. Lin, J.C. Zhang, J.J. Chang, Y. Hao, Realization of cost-effective and high-performance solar-blind ultraviolet PDs based on amorphous Ga_2O_3 prepared at room temperature. Mater. Today Adv. **16**, 100324 (2022). https://doi.org/10.1016/j.mtadv.2022.100324
76. T.C. Jiang, Y. Qiu, J. Tao, X. Xiao, Ga_2O_3@Al_2O_3 core–shell nanowires for high-performance solar-blind PDs. ACS Appl. Nano Mater. **6**, 9849 (2023). https://doi.org/10.1021/acsanm.3c01695
77. M.F. Wang, Z.Y. Hou, A.A.A. Kheraif, B.G. Xing, J. Lin, Mini review of TiO_2-based multifunctional nanocomposites for near-infrared light-responsive phototherapy. Adv. Healthc. Mater. **7**, 1800351 (2018). https://doi.org/10.1002/adhm.201800351
78. M.A.T. Arango, A.S.V.D. Andrade, D.T. Cipollone, L.O. Grant, K.A. Korakakis, Sierros, Robotic deposition of TiO_2 films on flexible substrates from hybrid inks: investigation of synthesis-processing-microstructure-photocatalytic relationships. ACS Appl. Mater. Interfaces **8**, 24659 (2016). https://doi.org/10.1021/acsami.6b05535
79. Y. Wang, P. Li, S.L. Chen, A.J. Wang, Dual-bandgap effect of photonic crystals on TiO_2 photocatalytic activity in ultraviolet and visible light regions. Catal. Surv. Asia **23**, 23 (2018). https://doi.org/10.1007/s10563-018-9259-0
80. M. Sendra, D. Sánchez-Quiles, J. Blasco, I. Moreno-Garrido, L.M. Lubián, S. Pérez-García, A. Tovar-Sánchez, Effects of TiO_2 nanoparticles and sunscreens on coastal marine microalgae: ultraviolet radiation is key variable for toxicity assessment. Environ. Int. **98**, 62 (2017). https://doi.org/10.1016/j.envint.2016.09.024
81. H.M. Tran, J.S. Bae, J. Hur, Self-powered, transparent, flexible, and solar-blind deep-UV detector based on surface-modified TiO_2 nanoparticles. Appl. Surf. Sci. **60**, 154528 (2022). https://doi.org/10.1016/j.apsusc.2022.154528
82. L.X. Su, Y. Zhu, D.Y. Yong, M.M. Chen, X. Ji, Y.Q. Su, X.C. Gui, B.C. Pan, R. Xiang, Z.K. Tang, Wide range bandgap modulation based on ZnO-based alloys and fabrication of solar blind UV detectors with high rejection ratio. ACS Appl. Mater. Interfaces **6**, 14152 (2014). https://doi.org/10.1021/am503427u
83. L.X. Su, Y. Zhu, Q.L. Zhang, M.M. Chen, T.Z. Wu, X.C. Gui, B.C. Pan, R. Xiang, Z.K. Tang, Structure and optical properties of ternary alloy BeZnO and quaternary alloy BeMgZnO films growth by molecular beam epitaxy. Appl. Surf. Sci. **274**, 341 (2013). https://doi.org/10.1016/j.apsusc.2013.03.058
84. L.X. Su, H.Y. Chen, X.J. Xu, X.S. Fang, Novel BeZnO based self-powered dual-color UV PD realized via a one-step fabrication method. Laser Photonics Rev. **11**, 1700222 (2017). https://doi.org/10.1002/lpor.201700222
85. C.H. Xu, L.L. Lan, Z. Wang, P.W. Lv, W. Zheng, Narrow-band solar-blind ultraviolet detectors based on AlSnO films with tunable band gap. ACS Appl. Mater. Interfaces **15**, 12017 (2023). https://doi.org/10.1021/acsami.2c20801
86. W. T. E, M. K. Li, D. X. Meng, Y. Cheng, W. Fu, P. Ye, Y. B. He, High-performance amorphous BeZnO-alloy-based solar-blind ultraviolet PDs on rigid and flexible substrates, J. Alloy Compd. **831**, 154819 (2020) https://doi.org/10.1016/j.jallcom.2020.154819
87. G.Y. Gou, G.Z. Dai, C. Qian, Y.F. Liu, Y. Fu, Z.Y. Tian, Y.K. He, L.G. Kong, J.L. Yang, J. Sun, Y.L. Gao, High-performance ultraviolet PDs based on CdS/CdS:SnS_2 superlattice nanowires. Nanoscale **8**, 14580 (2016). https://doi.org/10.1039/C6NR02915A
88. K. Park, J. Ah Lee, H. Soon Im, C.S. Jung, H.S. Kim, J. Park, C.L. Lee, GaP-ZnS pseudobinary alloy nanowires. Nano Lett. **14**, 5912 (2014). https://doi.org/10.1021/nl5028843
89. Q.Y. Bao, W.J. Li, P.Z. Xu, M. Zhang, D.X. Dai, P. Wang, X. Guo, L.M. Tong, On-chip single-mode CdS nanowire laser, Light: Sci. Appl. **9**, 42 (2020). https://doi.org/10.1038/s41377-020-0277-0
90. F.Z. Li, Y. Meng, R.T. Dong, S.P. Yip, C.Y. Lan, X.L. Kang, F.Y. Wang, K.S. Chan, J.C. Ho, High-performance transparent ultraviolet PDs based on InGaZnO superlattice nanowire arrays. ACS Nano **13**, 12042 (2019). https://doi.org/10.1021/acsnano.9b06311
91. Z. Lou, L.D. Li, G.Z. Shen, $InGaO_3$(ZnO) superlattice nanowires for high-performance ultraviolet PDs. Adv. Electron. Mater. **1**, 1500054 (2015). https://doi.org/10.1002/aelm.201500054
92. T. Zhang, F. Wang, P. Zhang, Y.F. Wang, H. Chen, J. Li, J. Wu, L. Chen, Z.D. Chen, S.B. Li, Low-temperature processed inorganic perovskites for flexible detectors with a broadband photoresponse. Nanoscale **11**, 2871 (2019). https://doi.org/10.1039/C8NR09900F

93. X.H. Wu, B.L. Zhou, J.C. Zhou, Y.T. Chen, Y.L. Chu, J. Huang, Distinguishable detection of ultraviolet, visible, and infrared spectrum with high-responsivity perovskite-based flexible photosensors. Small **14**, 1800527 (2018). https://doi.org/10.1002/smll.201800527
94. C.Y. Li, J. He, Y. Zhou, D.X. Qi, H. Jing, J. Su, R.W. Peng, R.H. Fan, P.V.C. Huo, T. Xu, M. Wang, Flexible perovskite nanosheet-based PDs for ultraviolet communication applications. Appl. Phys. Lett. **119**, 251105 (2021). https://doi.org/10.1063/5.0073706
95. H. Li, D.D. Yang, T. Zhang, P. Zhang, F. Wang, C.J. Qin, R.H. Yang, Z.D. Chen, S.B. Li, Flexible, UV-responsive perovskite PDs with low driving voltage. J. Mater. Sci. **54**, 11556 (2019). https://doi.org/10.1007/s10853-019-03721-3
96. G.G. Zhou, R. Sun, Y. Xiao, G. Abbas, Z.C. Peng, A high-performance flexible broadband PD based on graphene-PTAA-perovskite heterojunctions. Adv. Electron. Mater. **7**, 2000522 (2021). https://doi.org/10.1002/aelm.202000522
97. Y. Zhou, X. Qiu, Z.A. Wan, Z.H. Long, S. Poddar, Q.P. Zhang, Y.C. Ding, C.L.J. Chan, D.Q. Zhang, K. Zhou, Y.J. Lin, Z.Y. Fan, A Halide-exchanged perovskite PDs for wearable visible-blind ultraviolet monitoring. Nano Energy **100**, 107516 (2022). https://doi.org/10.1016/j.nanoen.2022.107516
98. S.L. Wang, Z.F. Zhu, Y.S. Zou, Y.H. Dong, S.T. Liu, J. Xue, L.M. Xu, Y.H. Dong, J.Z. Song, A low-dimension structure strategy for flexible PDs based on perovskite nanosheets/ZnO nanowires with broadband photoresponse. Sci. China Mater. **63**, 100 (2019). https://doi.org/10.1007/s40843-019-9441-6
99. J.H. Han, C.C. Liu, Y.Y. Zhang, Y. Guan, X. Zhang, W.J. Yu, Z.Y. Tang, Y.C. Liang, C.C. Wu, S.J. Zheng, L.X. Xiao, Quasi-2D ruddlesden–popper perovskites with low trap-states for high performance flexible self-powered ultraviolet PDs. Adv. Opt. Mater. **10**, 2201431 (2022). https://doi.org/10.1002/adom.202201431
100. I. Shtepliuk, R. Yakimova, Nature of photoexcited states in ZnO-embedded graphene quantum dots. Chem. Phys. **25**, 10525 (2023). https://doi.org/10.1039/D2CP04484F
101. X.M. Zhang, C.L. Yan, J.H. Yang, C. Pang, Y.Z. Yue, C.H. Zeng, B.S. Zhang, Vertical Schottky ultraviolet PD based on graphene and top–down fabricated GaN nanorod arrays. J. Semicond. **43**, 062804 (2022). https://doi.org/10.1088/1674-4926/43/6/062804
102. D.S. Liu, H.J. Li, J.R. Gao, S. Zhao, Y.K. Zhu, P. Wang, D. Wang, A.Y. Chen, X.Y. Wang, J.H. Yang, High-performance ultraviolet PD based on graphene quantum dots decorated ZnO nanorods/GaN film isotype heterojunctions. Nanoscale Res. Lett. **13**, 261 (2018). https://doi.org/10.1186/s11671-018-2672-5
103. C.S. Yin, J.H. Wu, J. Zhou, D.H. Zhang, Z.J. Liu, X.D. Liu, L.Z. Liu, Z.J. Zhan, S. Garner, Y.Q. Fu, Enhancing the sensitivity of flexible acoustic wave ultraviolet PD with graphene-quantum-dots decorated ZnO nanowires. Sens. Actuators, A **321**, 112590 (2021). https://doi.org/10.1016/j.sna.2021.112590
104. Y.L. Zheng, T. Tao, F.W. Sun, Q.H. Zheng, Flexible ultraviolet PD based ZnO film sputtered on paper. Vacuum **172**, 109089 (2020). https://doi.org/10.1016/j.vacuum.2019.109089
105. S.J. Vulić Tatjana, B. Zorić Dmitar, P. Marinković-Nedučin Radmila, The influence of the UV irradiation intensity on photocatalytic activity of ZnAl layered double hydroxides and derived mixed oxides. Chem. Ind. Chem. Eng. Q. **18**, 295 (2012). https://doi.org/10.2298/CICEQ110923006H
106. L.L. Liu, M. Cheng, Z.H. Yang, Improved performance of flower-like ZnAl LDH growing on carbon nanotubes used in zinc–nickel secondary battery. Electrochim. Acta **277**, 67 (2018). https://doi.org/10.1016/j.electacta.2018.04.201
107. G. Starukh, Photocatalytically enhanced cationic dye removal with Zn-Al layered double hydroxides. Nanoscale Res. Lett. **12**, 391 (2017). https://doi.org/10.1186/s11671-017-2173-y
108. H. Starukh, S. Levytska, The simultaneous anionic and cationic dyes removal with Zn Al layered double hydroxides. Appl. Clay Sci. **180**, 105183 (2019). https://doi.org/10.1016/j.clay.2019.105183
109. X.F. Zhao, L. Wang, X. Xu, X.D. Lei, S.L. Xu, F.Z. Zhang, Fabrication and photocatalytic properties of novel ZnO/$ZnAl_2O_4$ nanocomposite with $ZnAl_2O_4$ dispersed inside ZnO network. AIChE J. **58**, 573 (2012). https://doi.org/10.1002/aic.12597
110. A.M. Thomas, C.S. Yoon, S. Ippili, V. Jella, T.Y. Yang, G. Yoon, S.G. Yoon, High-performance flexible ultraviolet PDs based on facilely synthesized ecofriendly ZnAl:LDH nanosheets. ACS Appl. Mater. Interfaces **13**, 61434 (2021). https://doi.org/10.1021/acsami.1c19313
111. C.W. Jeon, S.S. Lee, I.K. Park, Flexible visible-blind ultraviolet PDs based on ZnAl-layered double hydroxide nanosheet scroll. ACS Appl. Mater. Interfaces **11**, 35138 (2019). https://doi.org/10.1021/acsami.9b12082
112. Y.Y. Peng, J.F. Lu, X.D. Wang, W.D. Ma, M.L. Que, Q.S. Chen, F.T. Li, X.H. Liu, E.W.C. Gao, F.C.F. Pan, Self-powered high-performance flexible GaN/ZnO heterostructure UV PDs with piezo-phototronic effect enhanced photoresponse. Nano Energy **94**, 106945 (2022). https://doi.org/10.1016/j.nanoen.2022.106945
113. J.M. Sun, C.C. Shan, M. Zhao, D.Y. Jiang, Research on piezo-phototronic effect in ZnO/AZO heterojunction flexible ultraviolet PDs. Optik **243**, 167472 (2021). https://doi.org/10.1016/j.ijleo.2021.167472
114. D.J. Lee, S.R. Ryu, G.M. Kumar, H.D. Cho, D.Y. Kim, P. Ilanchezhiyan, Piezo-phototronic effect triggered flexible UV PDs based on ZnO nanosheets/GaN nanorods arrays. Appl. Surf. Sci. **558**, 149896 (2021). https://doi.org/10.1016/j.apsusc.2021.149896
115. Y.M. Luo, B. Yin, H.Q. Zhang, Y. Qiu, J.X. Lei, Y. Chang, Y. Zhao, J.Y. Ji, L.Z. Hu, Piezoelectric effect enhancing decay time of p-NiO/n-ZnO ultraviolet PD. Appl. Surf. Sci. **361**, 157 (2016). https://doi.org/10.1016/j.apsusc.2015.11.158
116. G. Tian, D. Xiong, Y.H. Su, T. Yang, Y.Y. Gao, C. Yan, W. Deng, L. Jin, H.T. Zhang, X.Q. Fan, C.M. Wang, W.L. Deng, W.Q. Yang, Understanding the potential screening effect through the discretely structured ZnO nanorods piezo Array. Nano Lett. **20**, 4270 (2020). https://doi.org/10.1021/acs.nanolett.0c00793
117. Y. Wang, L.P. Zhu, Y.J. Feng, Z.N. Wang, Z.L. Wang, Comprehensive pyro-phototronic effect enhanced ultraviolet detector with ZnO/Ag schottky junction. Adv. Funct. Mater. **29**, 1807111 (2018). https://doi.org/10.1002/adfm.201807111
118. Y.H. Duan, M.Y. Cong, D.Y. Jiang, W. Zhang, X.J. Yang, C.C. Shan, X. Zhou, M. li, Q. Li, ZnO thin film flexible UV PDs: regulation on the ZnO/Au interface by piezo-phototronic effect and performance outcomes. Adv. Mater. Interfaces **6**, 1900470 (2019). https://doi.org/10.1002/admi.201900470
119. J.M. Sun, D.Y. Jiang, F.J. Zhang, Control of dual ultraviolet band flexible ultraviolet PD by piezo-phototronic effect. J. Lumin. **232**, 117875 (2021). https://doi.org/10.1016/j.jlumin.2020.117875
120. H. Wang, J. Ma, L. Cong, H. Zhou, P. Li, L. Fei, B. Li, H. Xu, Y. Liu, Piezoelectric effect enhanced flexible UV PD based on Ga_2O_3/ZnO heterojunction. Mater. Today Phys. **20**, 100464 (2021). https://doi.org/10.1016/j.mtphys.2021.100464
121. M.Y. Xue, W.B. Peng, X.F. Tang, Y.H. Cai, F.P. Li, Y.N. He, Pyro-phototronic effect enhanced pyramid structured p-Si/n-ZnO nanowires heterojunction PD. ACS Appl. Mater. Interfaces **15**, 4677 (2023). https://doi.org/10.1021/acsami.2c18011
122. J.Q. Dong, Z.J. Wang, X.F. Wang, Z.L. Wang, Temperature dependence of the pyro-phototronic effect in self-powered p-Si/n-ZnO nanowires heterojuncted ultraviolet sensors. Nano Today **29**, 100798 (2019). https://doi.org/10.1016/j.nantod.2019.100798

123. Y.L. Zhang, M.G. Hu, Z.N. Wang, Enhanced performances of p-si/n-ZnO self-powered PD by interface state modification and pyro-phototronic effect. Nano Energy **71**, 104630 (2020). https://doi.org/10.1016/j.nanoen.2020.104630
124. Y.M. Zhang, J. Chen, L.P. Zhu, Z.L. Wang, Self-powered high-responsivity PDs enhanced by the pyro-phototronic effect based on a $BaTiO_3$/GaN heterojunction. Nano Lett. **21**, 8808 (2021). https://doi.org/10.1021/acs.nanolett.1c03171
125. T.T. Nguyen, J. Kim, J. Yi, C.P. Wong, High-performing UV photodetectors by thermalcoupling transparent photovoltaics. Nano Energy **100**, 107504 (2022). https://doi.org/10.1016/j.nanoen.2022.107504
126. C.Y. Li, Y.C. Cai, Y.F. Xie, C.X. Sheng, Y.J. Qin, C.X. Cong, Z.J. Qiu, R. Liu, L.G. Hu, Enhanced dielectric/ferroelectric properties of PVDF-TrFE composite films with organic perovskite ferroelectrics. Mater. Today Phys. **16**, 031008 (2023). https://doi.org/10.35848/1882-0786/acc569
127. J. Chen, Z.H. Wang, H.F. He, J.X. Mao, Y. Zhang, Q.F. Zhang, M.K. Li, Y.M. Lu, Y.B. He, High-performance self-powered ultraviolet PD based on coupled ferroelectric depolarization field and heterojunction built-in potential. Adv. Electron. Mater **7**, 2100717 (2021). https://doi.org/10.1002/aelm.202100717
128. H.B. Wang, J.G. Ma, H. Chen, L.P. Wang, P. Li, Y.C. Liu, Ferroelectricity enhanced self-powered solar-blind UV PD based on Ga_2O_3/ZnO: V heterojunction. Mater. Today Phys. **30**, 100929 (2023). https://doi.org/10.1016/j.mtphys.2022.100929
129. X. Zhou, Q.Q. Ke, S. Tang, J.L. Luo, Z.H. Lu, Ultraviolet PDs based on ferroelectric depolarization field. J. Energy Chem. **77**, 487 (2023). https://doi.org/10.1016/j.jechem.2022.11.021
130. J. Huang, Q. Li, X.M. Lu, J.P. Meng, Z. Li, LSPR-enhanced pyro-phototronic effect for UV detection with an Ag-ZnO schottky junction device. Adv. Mater. Interfaces **9**, 2200327 (2022). https://doi.org/10.1002/admi.202200327
131. Q. Li, J.P. Meng, J. Huang, Z. Li, Plasmon-induced pyro-phototronic effect enhancement in self-powered UV-vis detection with a ZnO/CuO p-n junction device. Adv. Funct. Mater. **32**, 2108903 (2022). https://doi.org/10.1002/adfm.202108903
132. Q. Li, J. Huang, J.P. Meng, Z. Li, Enhanced performance of a self-powered ZnO photodetector by coupling LSPR-inspired pyro-phototronic effect and piezo-phototronic effect. Adv. Opt. Mater. **10**, 2102468 (2022). https://doi.org/10.1002/adom.202102468
133. J.Y. Huang, J.C. Jiang, L. Hu, Y.Y. Zeng, S.C. Ruan, Z.Z. Ye, Y.J. Zeng, Self-powered ultraviolet PD based on CuGaO/ZnSO heterojunction. J. Mater. Sci. **55**, 9003 (2020). https://doi.org/10.1007/s10853-020-04614-6
134. M.A. Yildirim, K. Teker, Self-powered fine-pattern flexible SiC single nanowire ultraviolet PD. J. Alloy. Compd. **868**, 159255 (2021). https://doi.org/10.1016/j.jallcom.2021.159255
135. B.D. Boruah, S.N. Majji, A. Misra, Surface photo-charge effect in doped-ZnO nanorods for high-performance self-powered ultraviolet PD. Nanoscale **9**, 4536 (2017). https://doi.org/10.1039/C6NR07670J
136. Y. Zhang, M.F. Peng, Y.N. Liu, T.T. Zhang, Q.Q. Zhu, H. Lei, S.N. Liu, Y. Tao, L. Li, Z. Wen, X.H. Sun, Flexible Self-powered real-Time ultraviolet PD by coupling triboelectric and photoelectric effects. ACS Appl. Mater. Interfaces **12**, 19384 (2020). https://doi.org/10.1021/acsami.9b22572
137. Z.H. Zhang, X.M. Li, J. Yin, Y. Xu, W.W. Fei, M.M. Xue, Q. Wang, J.X. Zhou, W.L. Guo, Emerging hydrovoltaic technology. Nat. Nanotechnol. **13**, 1109 (2018). https://doi.org/10.1038/s41565-018-0228-6
138. H.Y. Guan, G.J. Mao, T.Y. Zhong, T.M. Zhao, S. Liang, L.L. Xing, X.Y. Xue, A self-powered UV PD based on the hydrovoltaic and photoelectric coupling properties of ZnO nanowire arrays. J. Alloy. Compd. **867**, 159073 (2021). https://doi.org/10.1016/j.jallcom.2021.159073
139. S. Cai, X.J. Xu, W. Yang, J.X. Chen, X.S. Fang, Materials and designsfor wearable PDs. Adv. Mater. **31**, 1808138 (2019). https://doi.org/10.1002/adma.201808138
140. X.J. Xu, J.X. Chen, S. Cai, Z.H. Long, Y. Zhang, L.X. Su, S.S. He, C.Q. Tang, P. Liu, H.S. Peng, X.S. Fang, A real-time wearable UV-radiation monitor based on a high-performance p-CuZnS/n-TiO_2 PD. Adv. Mater. **30**, 1803165 (2018). https://doi.org/10.1002/adma.201803165
141. M.H. Tran, J. Hur, Ultrahigh stability of wearable photodetector using zirconium metal-organic framework enabling iIn situ and continuous monitoring of ultraviolet radiation risk. Adv. Opt. Mater. **10**, 2101404 (2021). https://doi.org/10.1002/adom.202101404
142. S.P.R. Mallem, P. Puneetha, D.Y. Lee, K.I. Park, D. Kim, S.J. An, J. Shim, Light-sensitive and strain-controlled flexible DNA/graphene/GaN bio-hybrid sensor based on the piezophototronic effect. Nano Energy **116**, 108807 (2023). https://doi.org/10.1016/j.nanoen.2023.108807